

## Incident-Field Excitation of the Line

---

The previous chapters have been devoted to the analysis of MTL's that are excited or driven by lumped sources in the termination networks. In this chapter we will examine the response of a MTL wherein the sources are electromagnetic fields incident on the line. These incident fields may be in the form of uniform plane waves such as are generated by distant transmitting antennas or they may be nonuniform fields such as are generated by nearby radiating structures. We will find that we may incorporate the effects of these incident fields by including distributed sources along the line. Once the MTL equations are derived from the resulting per-unit-length equivalent circuit, we concentrate on their solution.

### 7.1 DERIVATION OF THE MTL EQUATIONS FOR INCIDENT-FIELD EXCITATION

Incorporation of the effects of incident electromagnetic fields into the transmission-line equations was considered for two-conductor lines in [1–5]. This was later extended to multiconductor lines in [6–8] and [H.3–H.5]. A digital computer program has been developed for the multiconductor case [H.1, H.6]. The transmission-line formulation has been compared to the full-wave MOM solution in [H.2, H.7] and to experimental results in [H.8]. A literal solution for the two-wire case was obtained in [H.9]. The formulation has also been adapted to twisted pairs [9] and to shielded cables [10]. The derivation of the MTL equations follows essentially the same pattern as in Chapter 2.

The MTL equations which we will obtain will be solved and the termination networks incorporated into that general solution in the usual fashion in order to determine the line currents *at the ends of the line*. The currents that are modeled with these MTL equations are, once again, *differential-mode* or *transmission-line currents* in that the sum of the currents directed in the  $z$  direction on all  $(n + 1)$  conductors is zero at every line cross section. In other

words, the differential-mode currents of  $n$  of the conductors “return” on the reference conductor. In addition to these differential-mode currents, there can exist certain *common-mode* or *antenna-mode* currents that are not modeled by the MTL equations as discussed in Chapter 1 [3–5, 11–13]. So at points along the line there will be a combination of both currents only one component of which (the differential-mode) will be modeled by the MTL equations that we will develop. *If the MTL cross section is electrically small at the frequency of interest, the total current at the terminations is that predicted by the MTL equations.* This is because for a line with electrically small cross-sectional dimensions, we can surround each termination with a closed surface (approximately a “node” in lumped-circuit analysis terminology), and Kirchhoff’s current law shows that the total current entering this closed surface must be zero. Therefore at the terminations of a line having electrically small cross-sectional dimensions, the total current at the terminations must sum to zero (differential-mode or transmission-line current) so that the *common-mode current not predicted by the MTL equations must go to zero at the terminations* and is therefore of no importance in predicting the terminal responses of a MTL [13]. This also applies to crosstalk on MTL’s that have electrically small cross-sectional dimensions. Common-mode currents are important in modeling radiated emissions or for determining currents at some intermediate point along the line such as a folded dipole antenna [13]. Therefore the MTL equations we will obtain provide the complete prediction of the *terminal response* of a MTL which satisfies the necessary requirement of electrically small cross-sectional dimensions.

Consider an  $(n + 1)$ -conductor, uniform MTL where the conductors are parallel to the  $z$  axis as shown in Fig. 7.1. In order to derive the first MTL equation we again integrate Faraday’s law around the contour  $C_i$  between the reference conductor and the  $i$ -th conductor enclosing surface  $S_i$  in the clockwise direction as shown in Fig. 7.1:

$$\oint_{C_i} \vec{\mathcal{E}} \cdot d\vec{l} = \frac{d}{dt} \int_{S_i} \vec{\mathcal{B}} \cdot d\vec{s} \quad (7.1)$$

or

$$\int_a^{a'} \vec{\mathcal{E}}_i \cdot d\vec{l} + \int_{a'}^{b'} \vec{\mathcal{E}}_i \cdot d\vec{l} + \int_{b'}^b \vec{\mathcal{E}}_i \cdot d\vec{l} + \int_b^a \vec{\mathcal{E}}_i \cdot d\vec{l} = \frac{d}{dt} \int_{S_i} \vec{\mathcal{B}} \cdot \vec{a}_n ds \quad (7.2)$$

where  $\vec{\mathcal{E}}$  is the transverse electric field in the  $x$ - $y$  cross-sectional plane and  $\vec{\mathcal{E}}_i$  is the longitudinal or  $z$ -directed electric field along the surfaces of the conductors. Observe that again the negative sign is absent from the right-hand side of Faraday’s law because of the choice of the direction of the contour and the normal to the enclosed surface. At this point it is necessary to distinguish between *incident* and *scattered* field quantities. The incident field is that produced by the distant or nearby source *in the absence of the line conductors*. The scattered fields are produced by the currents and charges that are induced

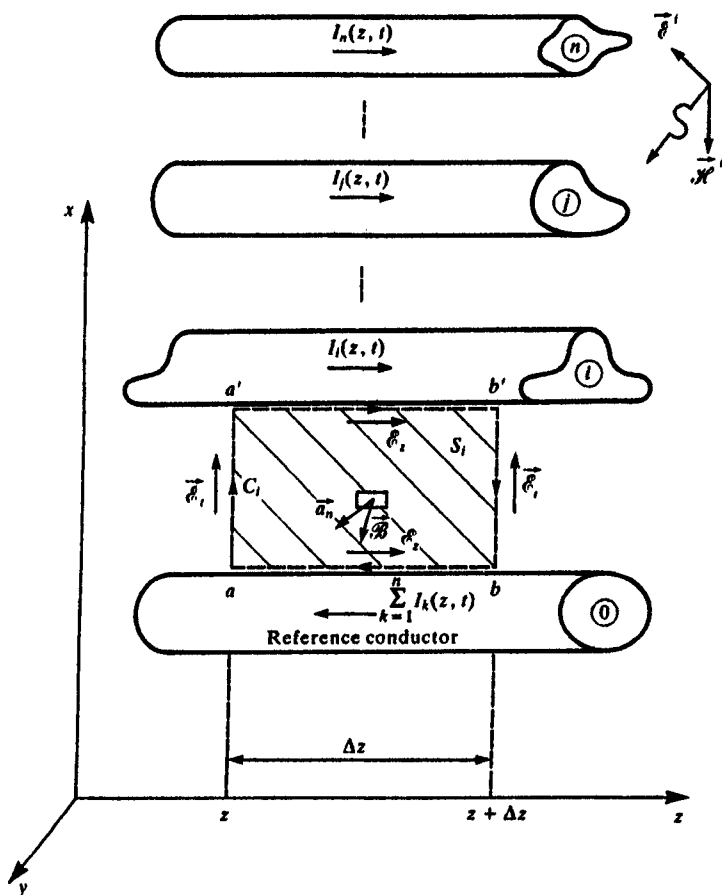


FIGURE 7.1 Definition of the contour for the derivation of the first MTL equation for incident-field illumination.

on the line conductors [6]. The total field is the sum of a scattered and an incident component as

$$\left. \begin{aligned} \vec{E}_i &= \vec{E}_i^i + \vec{E}_i^s \\ \vec{E}_o &= \vec{E}_o^i + \vec{E}_o^s \\ \vec{H} &= \vec{H}^i + \vec{H}^s \end{aligned} \right\} \quad (7.3)$$

where superscript *i* denotes *incident* and superscript *s* denotes *scattered*. There are some important assumptions that need to be stated. First we assume that the currents on the conductors are *z* directed. Therefore the scattered magnetic fields will lie entirely in the transverse plane. Since there is no *z*-directed  $\vec{H}^s$  field, Faraday's law shows that we may uniquely define the *scattered voltage*

between the  $i$ -th conductor and the reference conductor independent of path in the transverse plane as

$$V_i^s(z, t) = - \int_a^{a'} \vec{\mathcal{E}}_i^s \cdot d\vec{l} \quad (7.4a)$$

$$V_i^s(z + \Delta z, t) = - \int_b^{b'} \vec{\mathcal{E}}_i^s \cdot d\vec{l} \quad (7.4b)$$

Second, because of the transverse nature of the scattered magnetic field, the scattered magnetic field can be related to the currents that produced it with the usual per-unit-length inductances as

$$\lim_{\Delta z \rightarrow 0} \frac{1}{\Delta z} \int_{S_i} \vec{\mathcal{B}}^s \cdot \vec{a}_n ds = - [l_{i1} \quad \cdots \quad l_{ii} \quad \cdots \quad l_{in}] \begin{bmatrix} I_1(z, t) \\ \vdots \\ I_i(z, t) \\ \vdots \\ I_n(z, t) \end{bmatrix} \quad (7.5)$$

Let us represent the imperfect conductors with per-unit-length resistances,  $r_i$ . Although these will logically be functions of frequency due to the skin effect, let us for the moment assume they are constant with the assurance that the frequency-domain result will handle this dependence. The *total* longitudinal fields are related to the currents on the conductors as

$$\int_{a'}^{b'} \vec{\mathcal{E}}_i^s \cdot d\vec{l} = \int_{a'}^{b'} \mathcal{E}_z dz = r_i \Delta z I_i(z, t) \quad (7.6a)$$

$$\int_b^a \vec{\mathcal{E}}_i^s \cdot d\vec{l} = \int_b^a \mathcal{E}_z dz = r_0 \Delta z \sum_{k=1}^n I_k(z, t) \quad (7.6b)$$

Substituting (7.3), (7.4), (7.5), and (7.6) into (7.2), dividing by  $\Delta z$  and taking the limit as  $\Delta z \rightarrow 0$  yields

$$\frac{\partial}{\partial z} V_i^s(z, t) + [r_0 \quad \cdots \quad r_i + r_0 \quad \cdots \quad r_0] \begin{bmatrix} I_1(z, t) \\ \vdots \\ I_i(z, t) \\ \vdots \\ I_n(z, t) \end{bmatrix} \quad (7.7)$$

$$\begin{aligned}
 & + \frac{\partial}{\partial t} [l_{11} \quad \cdots \quad l_{1n} \quad \cdots \quad l_{nn}] \begin{bmatrix} I_1(z, t) \\ \vdots \\ I_n(z, t) \end{bmatrix} \\
 & = \frac{\partial}{\partial z} \int_a^{a'} \vec{\mathcal{E}}_i^l \cdot d\vec{l} + \frac{\partial}{\partial t} \int_a^{a'} \vec{\mathcal{B}}^l \cdot \vec{a}_n dl
 \end{aligned}$$

Repeating this for the other conductors and arranging in matrix form gives

$$\frac{\partial}{\partial z} \mathbf{V}^s(z, t) + \mathbf{R}\mathbf{I}(z, t) + \mathbf{L} \frac{\partial}{\partial t} \mathbf{I}(z, t) = \begin{bmatrix} \vdots \\ \frac{\partial}{\partial z} \int_a^{a'} \vec{\mathcal{E}}_i^l \cdot d\vec{l} + \frac{\partial}{\partial t} \int_a^{a'} \vec{\mathcal{B}}^l \cdot \vec{a}_n dl \\ \vdots \end{bmatrix} \quad (7.8)$$

This can be written in an alternative form by recognizing that the transverse and longitudinal electric fields and the normal magnetic fields are related by Faraday's law. This can be shown by writing Faraday's law around the contour in terms of the *incident* fields, given in (7.2), dividing both sides of the result by  $\Delta z$ , and taking the limit as  $\Delta z \rightarrow 0$  to give

$$\begin{aligned}
 \frac{\partial}{\partial z} \int_a^{a'} \vec{\mathcal{E}}_i^l \cdot d\vec{l} + \frac{\partial}{\partial t} \int_a^{a'} \vec{\mathcal{B}}^l \cdot \vec{a}_n \delta v &= \mathcal{E}_z^l(i\text{-th conductor}, z, t) \\
 &- \mathcal{E}_z^l(\text{reference conductor}, z, t)
 \end{aligned} \quad (7.9)$$

where  $\mathcal{E}_z^l(m\text{-th conductor}, z)$  is the longitudinal or  $z$ -directed *incident* electric field along the position of the  $m$ -th conductor *with it removed*. Substituting (7.9) into the right-hand side of (7.8) gives the first MTL equation:

$$\begin{aligned}
 \frac{\partial}{\partial z} \mathbf{V}^s(z, t) + \mathbf{R}\mathbf{I}(z, t) + \mathbf{L} \frac{\partial}{\partial t} \mathbf{I}(z, t) \\
 = \begin{bmatrix} \vdots \\ \mathcal{E}_z^l(i\text{-th conductor}, z, t) - \mathcal{E}_z^l(\text{reference conductor}, z, t) \\ \vdots \end{bmatrix}
 \end{aligned} \quad (7.10)$$

Observe that the voltages in this expression are the *scattered voltages* and not the *total voltages*.

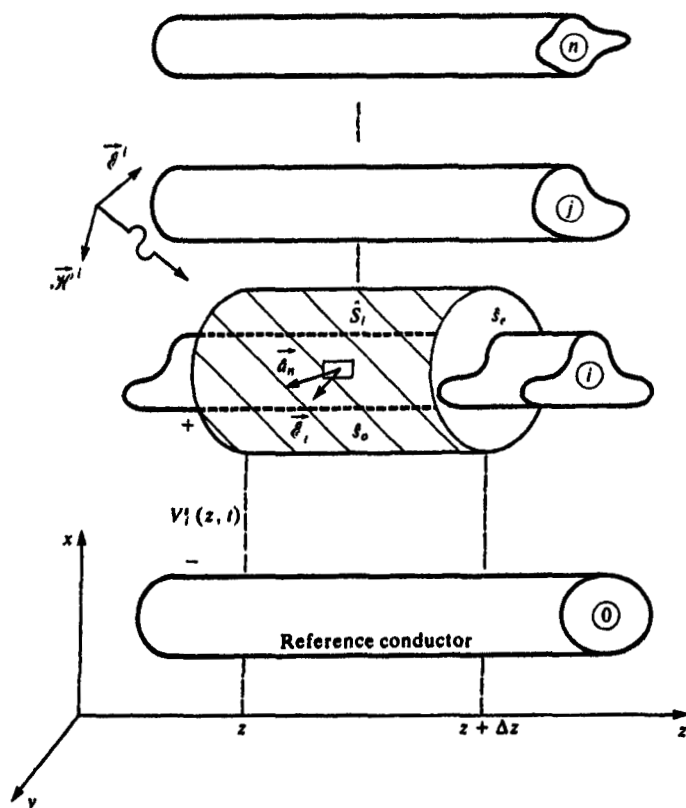


FIGURE 7.2 Definition of the surface for the derivation of the second MTL equation for incident-field illumination.

The second MTL equation can be derived as in Chapter 2 by enclosing the  $i$ -th conductor with a closed surface as illustrated in Fig. 7.2 and applying the continuity equation:

$$\oiint_{S_i} \vec{\mathcal{J}} \cdot d\vec{s} = -\frac{\partial}{\partial t} Q_{\text{enc}} \quad (7.11)$$

Over the end caps we have

$$\iint_{S_r} \vec{\mathcal{J}} \cdot d\vec{s} = I_i(z + \Delta z, t) - I_i(z, t) \quad (7.12)$$

Although there are some subtleties involved [6,8] we again define the per-unit-length conductance and capacitance matrices in terms of the *scattered* voltages as

$$I_{it}(z, t) = \lim_{\Delta z \rightarrow 0} \frac{1}{\Delta z} \iint_{\mathcal{S}_0} \vec{\mathcal{J}} \cdot d\vec{s} = \begin{bmatrix} -g_{i1} & \cdots & \sum_{k=1}^n g_{ik} & \cdots & -g_{in} \end{bmatrix} \begin{bmatrix} V_1^s(z, t) \\ \vdots \\ V_i^s(z, t) \\ \vdots \\ V_n^s(z, t) \end{bmatrix} \quad (7.13)$$

where  $I_{it}(z, t)$  is the transverse conduction current between the  $i$ -th conductor and all other conductors, and

$$\lim_{\Delta z \rightarrow 0} \frac{Q_{enc}}{\Delta z} = \begin{bmatrix} -c_{i1} & \cdots & \sum_{k=1}^n c_{ik} & \cdots & -c_{in} \end{bmatrix} \begin{bmatrix} V_1^s(z, t) \\ \vdots \\ V_i^s(z, t) \\ \vdots \\ V_n^s(z, t) \end{bmatrix} \quad (7.14)$$

Dividing both sides of (7.11) by  $\Delta z$ , taking the limit as  $\Delta z \rightarrow 0$ , and substituting (7.12), (7.13), and (7.14) yields the second MTL equation in matrix form as

$$\frac{\partial}{\partial z} \mathbf{I}(z, t) + \mathbf{G} \mathbf{V}^s(z, t) + \mathbf{C} \frac{\partial}{\partial t} \mathbf{V}^s(z, t) = \mathbf{0} \quad (7.15)$$

The above results are in terms of the *scattered voltages*. They can be placed in terms of the *total voltages* by writing

$$V_i(z, t) = V_i^i(z, t) + V_i^s(z, t) = V_i^i(z, t) - \int_a^{a'} \vec{\mathcal{E}}_i^i \cdot d\vec{l} \quad (7.16)$$

Substituting this into (7.8) and (7.15) gives the MTL equations in terms of the *total voltages* as

$$\frac{\partial}{\partial z} \mathbf{V}(z, t) + \mathbf{R} \mathbf{I}(z, t) + \mathbf{L} \frac{\partial}{\partial t} \mathbf{I}(z, t) = \frac{\partial}{\partial t} \begin{bmatrix} \vdots \\ \int_a^{a'} \vec{\mathcal{E}}^i \cdot d\vec{a}_n dl \\ \vdots \end{bmatrix} \quad (7.17a)$$

$$\frac{\partial}{\partial z} \mathbf{I}(z, t) + \mathbf{G} \mathbf{V}(z, t) + \mathbf{C} \frac{\partial}{\partial t} \mathbf{V}(z, t) = -\mathbf{G} \begin{bmatrix} \vdots \\ \int_a^{a'} \vec{\mathcal{E}}_i^i \cdot d\vec{l} \\ \vdots \end{bmatrix} - \mathbf{C} \frac{\partial}{\partial t} \begin{bmatrix} \vdots \\ \int_a^{a'} \vec{\mathcal{E}}_i^i \cdot d\vec{l} \\ \vdots \end{bmatrix} \quad (7.17b)$$

### 7.1.1 Equivalence of Source Representations

Evidently (7.17) shows that incident electromagnetic fields modify the MTL equations by adding *sources* to the usual homogeneous MTL equations. The MTL equations in terms of *total voltages* given in (7.17) can be written as

$$\frac{\partial}{\partial z} V(z, t) + RI(z, t) + L \frac{\partial}{\partial t} I(z, t) = V_F(z, t) \quad (7.18a)$$

$$\frac{\partial}{\partial z} I(z, t) + GV(z, t) + C \frac{\partial}{\partial t} V(z, t) = I_F(z, t) \quad (7.18b)$$

where

$$V_F(z, t) = \frac{\partial}{\partial t} \begin{bmatrix} \vdots \\ \int_a^{a'} \vec{\mathcal{E}}^i \cdot d\mathbf{l} \\ \vdots \end{bmatrix} \quad (7.19a)$$

$$I_F(z, t) = -G \begin{bmatrix} \vdots \\ \int_a^{a'} \vec{\mathcal{E}}_i^i \cdot d\mathbf{l} \\ \vdots \end{bmatrix} - C \frac{\partial}{\partial t} \begin{bmatrix} \vdots \\ \int_a^{a'} \vec{\mathcal{E}}_i^i \cdot d\mathbf{l} \\ \vdots \end{bmatrix} \quad (7.19b)$$

Thus the *sources* are the component of the incident magnetic field *normal* to the *i*-th circuit as shown in (7.19a) and the component of the incident electric field *transverse* to the *i*-th circuit as shown in (7.19b). Recall that the *i*-th circuit is the surface bounded by the *i*-th conductor and the reference conductor between *z* and *z* + Δ*z*. These MTL equations can be derived from the per-unit-length equivalent circuit shown in Fig. 7.3. This is the same as the previous circuits except that distributed sources are added to incorporate the incident-field source functions given in (7.19).

Observe that the right-hand side of (7.18a) depends on the incident magnetic field, whereas the right-hand side of (7.18b) depends on the incident electric field. These distributed “sources” can both be written in terms of only the *incident electric field* by using Faraday’s law in (7.9) to replace the incident magnetic field in  $V_F(z, t)$  to give

$$V_F(z, t) = \begin{bmatrix} \vdots \\ -\frac{\partial}{\partial z} \int_a^{a'} \vec{\mathcal{E}}_i^i \cdot d\mathbf{l} + \{ \mathcal{E}_x^i(i\text{-th conductor}, z, t) \\ - \mathcal{E}_x^i(\text{reference conductor}, z, t) \} \\ \vdots \end{bmatrix} \quad (7.19c)$$



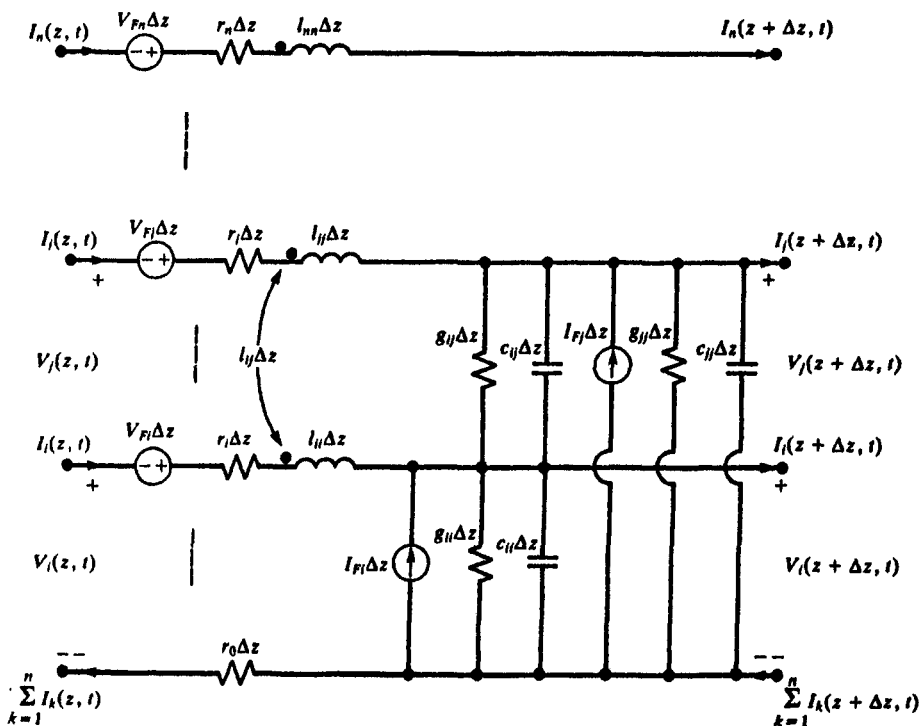


FIGURE 7.3 The per-unit-length equivalent circuit for a MTL with incident-field illumination.

On the other hand, in terms of the *scattered voltages*, the MTL equations become

$$\frac{\partial}{\partial z} \mathbf{V}^s(z, t) + \mathbf{R}\mathbf{I}(z, t) + \mathbf{L} \frac{\partial}{\partial t} \mathbf{I}(z, t) = \mathbf{V}_F^s(z, t) \quad (7.20a)$$

$$\frac{\partial}{\partial z} \mathbf{I}(z, t) + \mathbf{G}\mathbf{V}^s(z, t) + \mathbf{C} \frac{\partial}{\partial t} \mathbf{V}^s(z, t) = \mathbf{0} \quad (7.20b)$$

where

$$\mathbf{V}_F^s(z, t) = \begin{bmatrix} \vdots \\ \mathcal{E}_z^i(i\text{-th conductor}, z, t) - \mathcal{E}_z^i(\text{reference conductor}, z, t) \\ \vdots \end{bmatrix} \quad (7.21)$$

This latter form in terms of *scattered voltages* shows that the source term for the MTL equations is solely the difference in the incident electric field that is in the longitudinal direction and along the positions of the conductors (with them removed). It was shown above that these two forms are completely equivalent (although one of them uses the total voltages and the other uses the

scattered voltages). That these are equivalent is intuitive since Faraday's law essentially relates the net circulation of the electric field around a contour to the magnetic flux penetrating that contour.

There are some computational advantages to using (7.20) instead of (7.18) and converting the scattered voltages back to total voltages via (7.16):

$$V(z, t) = V_s^s(z, t) - \int_a^{a'} \vec{\mathcal{E}}_t^i \cdot d\vec{l} \quad (7.16)$$

However, there is a significant difference between the two forms when incorporating the terminal conditions. For example, suppose the terminal constraints are resistive with no lumped sources and are in the form of generalized Thévenin equivalents (incorporation of the terminal constraints will be addressed in more detail in Section 7.2.2):

$$V(0, t) = -R_S I(0, t) \quad (7.22a)$$

$$V(\mathcal{L}, t) = R_L I(\mathcal{L}, t) \quad (7.22b)$$

These can be used directly with the form of the MTL equations in (7.18) which are in terms of the *total voltages*. On the other hand, suppose we wish to use the form of the MTL equations in (7.20) which are in terms of *scattered voltages*. In this case, the appropriate terminal constraints must be in terms of the scattered voltages. To obtain these we substitute (7.16) into (7.22a) and (7.22b) to yield

$$V^s(0, t) = \left[ \begin{array}{c} \vdots \\ \int_a^{a'} \vec{\mathcal{E}}_t^i \cdot d\vec{l} \\ \vdots \end{array} \right]_{z=0} - R_S I(0, t) \quad (7.22c)$$

$$V^s(\mathcal{L}, t) = \left[ \begin{array}{c} \vdots \\ \int_a^{a'} \vec{\mathcal{E}}_t^i \cdot d\vec{l} \\ \vdots \end{array} \right]_{z=\mathcal{L}} + R_L I(\mathcal{L}, t) \quad (7.22d)$$

Therefore when we use the formulation in terms of scattered voltages, the driving sources in the MTL equations are simply the longitudinal incident electric fields but the integrals of the transverse incident electric field are nevertheless included in the results since they appear as sources in the terminations as shown by (7.22). This important subtlety is frequently overlooked and leads to incorrect results for the terminal currents and voltages as well as controversy over the proper form of the incident-field-excitation sources. When this is observed, equivalent results for the terminal voltages and currents will

be obtained with either of the forms of the incident field excitation: (7.18) or (7.20). Throughout this chapter we will use the form in terms of the *total voltage* given in (7.18) with the source vectors given in (7.19).

## 7.2 FREQUENCY-DOMAIN SOLUTIONS

In the frequency domain the phasor MTL equations become

$$\frac{d}{dz} \hat{\mathbf{V}}(z) = -\hat{\mathbf{Z}}\hat{\mathbf{I}}(z) + \hat{\mathbf{V}}_F(z) \quad (7.23a)$$

$$\frac{d}{dz} \hat{\mathbf{I}}(z) = -\hat{\mathbf{Y}}\hat{\mathbf{V}}(z) + \hat{\mathbf{I}}_F(z) \quad (7.23b)$$

where

$$\hat{\mathbf{Z}} = \mathbf{R} + j\omega\mathbf{L} \quad (7.24a)$$

$$\hat{\mathbf{Y}} = \mathbf{G} + j\omega\mathbf{C} \quad (7.24b)$$

and

$$\hat{\mathbf{V}}_F(z) = j\omega \begin{bmatrix} \vdots \\ \int_a^{a'} \tilde{\mathbf{B}}^t \cdot \hat{\mathbf{a}}_n dl \\ \vdots \end{bmatrix} \quad (7.24c)$$

$$\hat{\mathbf{I}}_F(z) = -\hat{\mathbf{Y}} \begin{bmatrix} \vdots \\ \int_a^{a'} \tilde{\mathbf{E}}_i^t \cdot d\mathbf{l} \\ \vdots \end{bmatrix} \quad (7.24d)$$

Alternatively, the forcing function  $\hat{\mathbf{V}}_F(z)$  can be written in terms of the incident electric field as in (7.19c) as

$$\hat{\mathbf{V}}_F(z) = \begin{bmatrix} \vdots \\ -\frac{\partial}{\partial z} \int_a^{a'} \tilde{\mathbf{E}}_i^t \cdot d\mathbf{l} + \{ \hat{\mathbf{E}}_z^t(l\text{-th conductor}, z) \\ - \hat{\mathbf{E}}_z^t(\text{reference conductor}, z) \} \\ \vdots \end{bmatrix} \quad (7.24e)$$

Once again these can be written in state-variable form as a coupled set of

first-order, ordinary differential equations in matrix form as

$$\underbrace{\frac{d}{dz} \begin{bmatrix} \hat{\mathbf{V}}(z) \\ \hat{\mathbf{I}}(z) \end{bmatrix}}_{\hat{\mathbf{X}}(z)} = \underbrace{\begin{bmatrix} \mathbf{0} & -\hat{\mathbf{Z}} \\ -\hat{\mathbf{Y}} & \mathbf{0} \end{bmatrix}}_{\hat{\mathbf{A}}} \underbrace{\begin{bmatrix} \hat{\mathbf{V}}(z) \\ \hat{\mathbf{I}}(z) \end{bmatrix}}_{\hat{\mathbf{X}}(z)} + \begin{bmatrix} \hat{\mathbf{V}}_F(z) \\ \hat{\mathbf{I}}_F(z) \end{bmatrix} \quad (7.25)$$

There are considerable advantages in writing the phasor MTL equations in this form as we show in the next section. In fact, drawing from the wealth of properties of the analogous solution for lumped, linear systems, we can immediately write the solution to these phasor MTL equations.

### 7.2.1 Solution of the MTL Equations

The solution to the phasor MTL equations given in (7.25) can again be immediately obtained by observing that they are directly analogous to the state-variable equations for lumped systems discussed in Chapter 4 [A.2, B.1, H.3]:

$$\frac{d}{dt} \mathbf{X}(t) = \mathbf{A}\mathbf{X}(t) + \mathbf{B}\mathbf{W}(t) \quad (7.26)$$

The solution to these state-variable equations was discussed in Chapter 4 and becomes

$$\mathbf{X}(t) = \Phi(t - t_0)\mathbf{X}(t_0) + \int_{t_0}^t \Phi(t - \tau)\mathbf{B}\mathbf{W}(\tau) d\tau \quad (7.27a)$$

where the *state-transition matrix* is

$$\Phi(t_2 - t_1) \equiv e^{\mathbf{A}(t_2 - t_1)} \quad (7.27b)$$

Therefore, the solution to the phasor MTL equations in (7.25) becomes, by direct analogy,

$$\hat{\mathbf{X}}(z) = \hat{\Phi}(z - z_0)\hat{\mathbf{X}}(z_0) + \int_{z_0}^z \hat{\Phi}(z - \tau) \begin{bmatrix} \hat{\mathbf{V}}_F(\tau) \\ \hat{\mathbf{I}}_F(\tau) \end{bmatrix} d\tau \quad (7.28a)$$

where

$$\hat{\mathbf{X}}(z) = \begin{bmatrix} \hat{\mathbf{V}}(z) \\ \hat{\mathbf{I}}(z) \end{bmatrix} \quad (7.28b)$$

and the *chain parameter matrix* is defined as

$$\begin{aligned}\hat{\Phi}(z) &\equiv e^{\hat{\Lambda}z} \\ &= \begin{bmatrix} \hat{\Phi}_{11}(z) & \hat{\Phi}_{12}(z) \\ \hat{\Phi}_{21}(z) & \hat{\Phi}_{22}(z) \end{bmatrix}\end{aligned}\quad (7.28c)$$

The  $n \times n$  submatrices of the chain parameter matrix,  $\hat{\Phi}_{ij}(z)$ , are given in (4.70):

$$\hat{\Phi}_{11}(\mathcal{L}) = \frac{1}{2}\hat{\mathbf{Y}}^{-1}\hat{\mathbf{T}}(\mathbf{e}^{j\mathcal{L}} + \mathbf{e}^{-j\mathcal{L}})\hat{\mathbf{T}}^{-1}\hat{\mathbf{Y}} \quad (4.70a)$$

$$\hat{\Phi}_{12}(\mathcal{L}) = -\frac{1}{2}\hat{\mathbf{Y}}^{-1}\hat{\mathbf{T}}\hat{\gamma}(\mathbf{e}^{j\mathcal{L}} - \mathbf{e}^{-j\mathcal{L}})\hat{\mathbf{T}}^{-1} \quad (4.70b)$$

$$\hat{\Phi}_{21}(\mathcal{L}) = -\frac{1}{2}\hat{\mathbf{T}}(\mathbf{e}^{j\mathcal{L}} - \mathbf{e}^{-j\mathcal{L}})\hat{\gamma}^{-1}\hat{\mathbf{T}}^{-1}\hat{\mathbf{Y}} \quad (4.70c)$$

$$\hat{\Phi}_{22}(\mathcal{L}) = \frac{1}{2}\hat{\mathbf{T}}(\mathbf{e}^{j\mathcal{L}} + \mathbf{e}^{-j\mathcal{L}})\hat{\mathbf{T}}^{-1} \quad (4.70d)$$

where  $\mathbf{T}^{-1}\mathbf{Y}\mathbf{Z}\mathbf{T} = \hat{\gamma}^2$ .

Observe in (7.28a) that the incident fields add a *convolution* term to the usual chain parameter relation. Writing (7.28a) out for a MTL of total length  $\mathcal{L}$  gives

$$\begin{bmatrix} \hat{\mathbf{V}}(\mathcal{L}) \\ \hat{\mathbf{I}}(\mathcal{L}) \end{bmatrix} = \begin{bmatrix} \hat{\Phi}_{11}(\mathcal{L}) & \hat{\Phi}_{12}(\mathcal{L}) \\ \hat{\Phi}_{21}(\mathcal{L}) & \hat{\Phi}_{22}(\mathcal{L}) \end{bmatrix} \begin{bmatrix} \hat{\mathbf{V}}(0) \\ \hat{\mathbf{I}}(0) \end{bmatrix} + \begin{bmatrix} \hat{\mathbf{V}}_{FT}(\mathcal{L}) \\ \hat{\mathbf{I}}_{FT}(\mathcal{L}) \end{bmatrix} \quad (7.29a)$$

where the total source voltages  $\hat{\mathbf{V}}_{FT}(\mathcal{L})$  and  $\hat{\mathbf{I}}_{FT}(\mathcal{L})$  are, according to (7.28a),

$$\hat{\mathbf{V}}_{FT}(\mathcal{L}) = \int_0^{\mathcal{L}} [\hat{\Phi}_{11}(\mathcal{L} - \tau)\hat{\mathbf{V}}_F(\tau) + \hat{\Phi}_{12}(\mathcal{L} - \tau)\hat{\mathbf{I}}_F(\tau)] d\tau \quad (7.29b)$$

$$\hat{\mathbf{I}}_{FT}(\mathcal{L}) = \int_0^{\mathcal{L}} [\hat{\Phi}_{21}(\mathcal{L} - \tau)\hat{\mathbf{V}}_F(\tau) + \hat{\Phi}_{22}(\mathcal{L} - \tau)\hat{\mathbf{I}}_F(\tau)] d\tau \quad (7.29c)$$

According to (7.29a) the equivalent circuit of the complete line can be viewed as an unexcited line in series with the equivalent sources  $\hat{\mathbf{V}}_{FT}(\mathcal{L})$  and  $\hat{\mathbf{I}}_{FT}(\mathcal{L})$  located at  $z = \mathcal{L}$  as illustrated in Fig. 7.4.

**7.2.1.1 Simplified Forms of the Excitations** The total excitation source vectors due to the incident field,  $\hat{\mathbf{I}}_{FT}(\mathcal{L})$  and  $\hat{\mathbf{V}}_{FT}(\mathcal{L})$ , in (7.29b) and (7.29c) can be simplified using the definitions of the phasor distributed sources,  $\hat{\mathbf{I}}_F(z)$  and  $\hat{\mathbf{V}}_F(z)$ , given in (7.24d) and (7.24e) and the properties of the chain parameter submatrices obtained in Section 4.3.3. The total forcing function,  $\hat{\mathbf{V}}_{FT}(\mathcal{L})$ , given in (7.29b) becomes, by substituting  $\hat{\mathbf{I}}_F(z)$  from (7.24d) and  $\hat{\mathbf{V}}_F(z)$  from (7.24e),

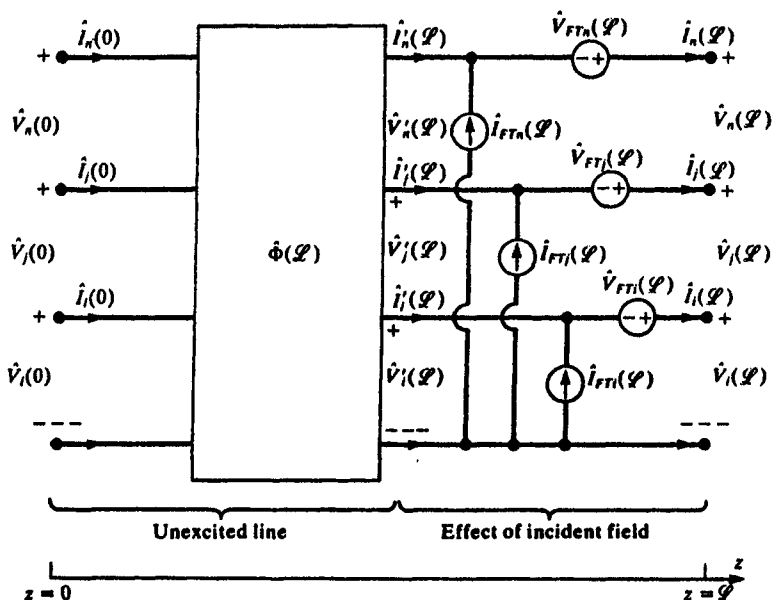


FIGURE 7.4 Illustration of the representation of a MTL with incident-field illumination as a  $2n$  port having lumped sources that represent the effects of the incident field.

$$\hat{V}_{FT}(\mathcal{L}) = \int_0^{\mathcal{L}} [\hat{\Phi}_{11}(\mathcal{L} - \tau) \hat{V}_F(\tau) + \hat{\Phi}_{12}(\mathcal{L} - \tau) \hat{\mathbf{I}}_F(\tau)] d\tau \quad (7.30)$$

$$= \int_0^{\mathcal{L}} \hat{\Phi}_{11}(\mathcal{L} - \tau) \begin{bmatrix} \vdots \\ \hat{E}_z^i(i\text{-th conductor}, \tau) \\ -\hat{E}_z^i(\text{reference conductor}, \tau) \\ \vdots \end{bmatrix} d\tau$$

$$- \int_0^{\mathcal{L}} \hat{\Phi}_{11}(\mathcal{L} - \tau) \frac{\partial}{\partial \tau} \begin{bmatrix} \vdots \\ \int_a^{a'} \tilde{\mathbf{E}}_i^i \cdot d\mathbf{l} \\ \vdots \end{bmatrix} d\tau$$

$$- \int_0^{\mathcal{L}} \hat{\Phi}_{12}(\mathcal{L} - \tau) \hat{\mathbf{Y}} \begin{bmatrix} \vdots \\ \int_a^{a'} \tilde{\mathbf{E}}_i^i \cdot d\mathbf{l} \\ \vdots \end{bmatrix} d\tau$$

Using the chain rule for differentiation:

$$\frac{\partial}{\partial \tau} [A(\tau)B(\tau)] = A(\tau) \left[ \frac{\partial}{\partial \tau} B(\tau) \right] + \left[ \frac{\partial}{\partial \tau} A(\tau) \right] B(\tau) \quad (7.31)$$

we obtain

$$\begin{aligned} \hat{V}_{FT}(\mathcal{L}) = & \int_0^{\mathcal{L}} \hat{\Phi}_{11}(\mathcal{L} - \tau) \begin{bmatrix} \vdots \\ \hat{E}_i^l(i\text{-th conductor}, \tau) \\ -\hat{E}_i^l(\text{reference conductor}, \tau) \\ \vdots \end{bmatrix} d\tau \quad (7.32) \\ & - \int_0^{\mathcal{L}} \frac{\partial}{\partial \tau} \left\{ \hat{\Phi}_{11}(\mathcal{L} - \tau) \begin{bmatrix} \vdots \\ \int_a^{a'} \tilde{E}_i^l \cdot d\tilde{l} \\ \vdots \end{bmatrix} \right\} d\tau \\ & + \int_0^{\mathcal{L}} \left\{ \underbrace{\frac{\partial}{\partial \tau} \hat{\Phi}_{11}(\mathcal{L} - \tau) - \hat{\Phi}_{12}(\mathcal{L} - \tau) \hat{Y}}_{=0} \right\} \begin{bmatrix} \vdots \\ \int_a^{a'} \tilde{E}_i^l \cdot d\tilde{l} \\ \vdots \end{bmatrix} d\tau \end{aligned}$$

We now show that the last term in (7.32) is identically zero, i.e.,

$$\frac{\partial}{\partial \tau} \hat{\Phi}_{11}(\mathcal{L} - \tau) - \hat{\Phi}_{12}(\mathcal{L} - \tau) \hat{Y} = 0 \quad (7.33)$$

This can be easily shown using the chain parameter submatrix definitions given in (4.70):

$$\frac{\partial}{\partial \tau} \hat{\Phi}_{11}(\mathcal{L} - \tau) = \frac{\partial}{\partial \tau} [\tfrac{1}{2} \hat{Y}^{-1} \hat{T}(e^{\mathcal{H}(\mathcal{L}-\tau)} + e^{-\mathcal{H}(\mathcal{L}-\tau)}) \hat{T}^{-1} \hat{Y}] \quad (7.34a)$$

$$= -\tfrac{1}{2} \hat{Y}^{-1} \hat{T} \hat{\gamma}(e^{\mathcal{H}(\mathcal{L}-\tau)} - e^{-\mathcal{H}(\mathcal{L}-\tau)}) \hat{T}^{-1} \hat{Y}$$

$$- \hat{\Phi}_{12}(\mathcal{L} - \tau) \hat{Y} = \tfrac{1}{2} \hat{Y}^{-1} \hat{T} \hat{\gamma}(e^{\mathcal{H}(\mathcal{L}-\tau)} - e^{-\mathcal{H}(\mathcal{L}-\tau)}) \hat{T}^{-1} \hat{Y} \quad (7.34b)$$

Thus the final result is

$$\hat{V}_{FT}(\mathcal{L}) = \int_0^{\mathcal{L}} \hat{\Phi}_{11}(\mathcal{L} - \tau) \begin{bmatrix} \vdots \\ \hat{E}_i^l(i\text{-th conductor}, \tau) \\ -\hat{E}_i^l(\text{reference conductor}, \tau) \\ \vdots \end{bmatrix} d\tau \quad (7.35)$$

$$-\underbrace{\hat{\Phi}_{11}(0)}_{1_n} \begin{bmatrix} \vdots \\ \int_a^{a'} \tilde{\mathbf{E}}_i^t \cdot d\mathbf{l} \\ \vdots \end{bmatrix}_{z=\mathcal{L}} + \hat{\Phi}_{11}(\mathcal{L}) \begin{bmatrix} \vdots \\ \int_a^{a'} \tilde{\mathbf{E}}_i^t \cdot d\mathbf{l} \\ \vdots \end{bmatrix}_{z=0}$$

where we have used the fact that  $\hat{\Phi}_{11}(0) = 1_n$  where  $1_n$  is the  $n \times n$  identity matrix. In a similar fashion we can show that

$$\begin{aligned} \hat{\mathbf{I}}_{FT}(\mathcal{L}) = \int_0^{\mathcal{L}} \hat{\Phi}_{21}(\mathcal{L} - \tau) & \begin{bmatrix} \vdots \\ \hat{\mathbf{E}}_s^t(i\text{-th conductor}, \tau) \\ -\hat{\mathbf{E}}_s^t(\text{reference conductor}, \tau) \\ \vdots \end{bmatrix} d\tau \quad (7.36) \\ & - \underbrace{\hat{\Phi}_{21}(0)}_0 \begin{bmatrix} \vdots \\ \int_a^{a'} \tilde{\mathbf{E}}_i^t \cdot d\mathbf{l} \\ \vdots \end{bmatrix}_{z=\mathcal{L}} + \hat{\Phi}_{21}(\mathcal{L}) \begin{bmatrix} \vdots \\ \int_a^{a'} \tilde{\mathbf{E}}_s^t \cdot d\mathbf{l} \\ \vdots \end{bmatrix}_{z=0} \end{aligned}$$

where we have used the property that  $\hat{\Phi}_{21}(0) = 0$  (see (4.70c)). These results show that the total forcing functions,  $\hat{\mathbf{V}}_{FT}(\mathcal{L})$  and  $\hat{\mathbf{I}}_{FT}(\mathcal{L})$ , depend on a *convolution* of one of the chain parameter submatrices and the longitudinal incident electric field along the positions of the conductors (with them removed) as well as the product of that chain parameter submatrix and the integrals of the transverse incident electric field (with the conductors removed) which are evaluated at the left end of the line ( $z = 0$ ) and at the right end of the line ( $z = \mathcal{L}$ ). These forms are simpler to evaluate than those in (7.29).

The important simplifications of the total forcing functions,  $\hat{\mathbf{V}}_{FT}(\mathcal{L})$  and  $\hat{\mathbf{I}}_{FT}(\mathcal{L})$ , given in (7.35) and (7.36) can also be derived in a different fashion if we are careful to recall the distinction between *total* and *scattered* voltages given in (7.16). The solution for the form of the MTL equations in terms of *scattered* voltages given in (7.20) can be similarly obtained using the state-variable equation result given in (7.28). In that result the forcing functions become  $\hat{\mathbf{V}}_F(\tau) \Rightarrow \hat{\mathbf{V}}_F^s(\tau)$  and  $\hat{\mathbf{I}}_F(\tau) \Rightarrow \hat{\mathbf{I}}_F^s(\tau) = 0$  and the line voltage is the scattered voltage,  $\hat{\mathbf{V}}(z) \Rightarrow \hat{\mathbf{V}}^s(z)$ . Writing out the solution in (7.29) and substituting the relation between scattered and total voltages in (7.16) yields the simplified forms of the total forcing functions given in (7.35) and (7.36).

## 7.2.2 Incorporation of the Terminal Conditions

Now that the general solution of the phasor MTL equations has been obtained in terms of the chain parameter matrix and the incident-field forcing functions,



we next incorporate the terminal conditions to arrive at an explicit solution for the phasor line voltages and currents. Consider Fig. 7.4. The voltages and currents at the right end of the unexcited line are denoted as  $\hat{V}'(\mathcal{L})$  and  $\hat{I}'(\mathcal{L})$ . These are related to the actual desired voltages and currents,  $\hat{V}(\mathcal{L})$  and  $\hat{I}(\mathcal{L})$ , as

$$\hat{V}'(\mathcal{L}) = \hat{V}(\mathcal{L}) - \hat{V}_{FT}(\mathcal{L}) \quad (7.37a)$$

$$\hat{I}'(\mathcal{L}) = \hat{I}(\mathcal{L}) - \hat{I}_{FT}(\mathcal{L}) \quad (7.37b)$$

Therefore, we can incorporate the effects of incident fields into the solution by replacing  $\hat{V}(\mathcal{L})$  and  $\hat{I}(\mathcal{L})$  in the equations for the terminal responses without incident field illumination given in Section 4.3.5 with  $\hat{V}(\mathcal{L}) - \hat{V}_{FT}(\mathcal{L})$  and  $\hat{I}(\mathcal{L}) - \hat{I}_{FT}(\mathcal{L})$ ! This is further confirmed by rewriting the general solution given in (7.29a) in terms of the chain parameter matrix with sources. Rewriting this in the form of the chain parameter relation *without incident-field illumination* gives

$$\begin{bmatrix} \hat{V}(\mathcal{L}) - \hat{V}_{FT}(\mathcal{L}) \\ \hat{I}(\mathcal{L}) - \hat{I}_{FT}(\mathcal{L}) \end{bmatrix} = \begin{bmatrix} \hat{\Phi}_{11}(\mathcal{L}) & \hat{\Phi}_{12}(\mathcal{L}) \\ \hat{\Phi}_{21}(\mathcal{L}) & \hat{\Phi}_{22}(\mathcal{L}) \end{bmatrix} \begin{bmatrix} \hat{V}(0) \\ \hat{I}(0) \end{bmatrix} \quad (7.38)$$

Consider the terminal conditions written in the form of generalized Thévenin equivalents as

$$\hat{V}(0) = \hat{V}_s - \hat{Z}_s \hat{I}(0) \quad (7.39a)$$

$$\hat{V}(\mathcal{L}) = \hat{V}_L + \hat{Z}_L \hat{I}(\mathcal{L}) \quad (7.39b)$$

Making the substitutions in (7.37) gives

$$\hat{V}(0) = \hat{V}_s - \hat{Z}_s \hat{I}(0) \quad (7.40a)$$

$$[\hat{V}'(\mathcal{L}) + \hat{V}_{FT}(\mathcal{L})] = \hat{V}_L + \hat{Z}_L [\hat{I}'(\mathcal{L}) + \hat{I}_{FT}(\mathcal{L})] \quad (7.40b)$$

or

$$\hat{V}(0) = \hat{V}_s - \hat{Z}_s \hat{I}(0) \quad (7.41a)$$

$$\hat{V}'(\mathcal{L}) = [\hat{V}_L - \hat{V}_{FT}(\mathcal{L}) + \hat{Z}_L \hat{I}_{FT}(\mathcal{L})] + \hat{Z}_L \hat{I}'(\mathcal{L}) \quad (7.41b)$$

Observe that (7.41) shows we could modify (4.90) for no incident-field illumination by replacing  $\hat{V}_L$  with  $\hat{V}_L - \hat{V}_{FT}(\mathcal{L}) + \hat{Z}_L \hat{I}_{FT}(\mathcal{L})$  and  $\hat{I}(\mathcal{L})$  with  $\hat{I}(\mathcal{L}) - \hat{I}_{FT}(\mathcal{L})$  to yield

$$[\hat{\Phi}_{11} \hat{Z}_s + \hat{Z}_L \hat{\Phi}_{22} - \hat{\Phi}_{12} - \hat{Z}_L \hat{\Phi}_{21} \hat{Z}_s] \hat{I}(0) \quad (7.42a)$$

$$= \underbrace{[\hat{\Phi}_{11} - \hat{Z}_L \hat{\Phi}_{21}] \hat{V}_s - \hat{V}_L}_{\text{due to lumped sources}} + \underbrace{[\hat{V}_{FT}(\mathcal{L}) - \hat{Z}_L \hat{I}_{FT}(\mathcal{L})]}_{\text{due to incident field}}$$

$$\hat{I}(\mathcal{L}) = \hat{I}_{FT}(\mathcal{L}) + \hat{\Phi}_{21} \hat{V}_s + [\hat{\Phi}_{22} - \hat{\Phi}_{21} \hat{Z}_s] \hat{I}(0) \quad (7.42b)$$

Similarly, the alternative result given in (4.88) becomes

$$\begin{bmatrix} (\hat{Z}_C + \hat{Z}_S)\hat{T} & (\hat{Z}_C - \hat{Z}_S)\hat{T} \\ (\hat{Z}_C - \hat{Z}_L)\hat{T}e^{-\gamma\mathcal{L}} & (\hat{Z}_C + \hat{Z}_L)\hat{T}e^{\gamma\mathcal{L}} \end{bmatrix} \begin{bmatrix} \hat{I}_m^+ \\ \hat{I}_m^- \end{bmatrix} = \begin{bmatrix} \hat{V}_S \\ \hat{V}_L - \hat{V}_{FT}(\mathcal{L}) + \hat{Z}_L \hat{I}_{FT}(\mathcal{L}) \end{bmatrix} \quad (7.43)$$

where the characteristic impedance matrix is  $\hat{Z}_C = \hat{Z}\hat{T}\hat{\gamma}^{-1}\mathbf{T}^{-1} = \hat{\mathbf{Y}}^{-1}\hat{T}\hat{\gamma}\mathbf{T}^{-1}$ . The solutions for the terminal voltages so obtained will be

$$\hat{V}(0) = \hat{\mathbf{Y}}^{-1}\hat{T}\hat{\gamma}(\hat{I}_m^+ + \hat{I}_m^-) \quad (7.44a)$$

$$= \hat{Z}\hat{T}\hat{\gamma}^{-1}(\hat{I}_m^+ + \hat{I}_m^-)$$

$$\hat{V}'(\mathcal{L}) = \hat{V}(\mathcal{L}) - \hat{V}_{FT}(\mathcal{L}) \quad (7.44b)$$

$$= \hat{\mathbf{Y}}^{-1}\hat{T}\hat{\gamma}(e^{-\gamma\mathcal{L}}\hat{I}_m^+ + e^{\gamma\mathcal{L}}\hat{I}_m^-)$$

$$= \hat{Z}\hat{T}\hat{\gamma}^{-1}(e^{-\gamma\mathcal{L}}\hat{I}_m^+ + e^{\gamma\mathcal{L}}\hat{I}_m^-)$$

or

$$\hat{V}(\mathcal{L}) = \hat{V}_{FT}(\mathcal{L}) + \hat{\mathbf{Y}}^{-1}\hat{T}\hat{\gamma}(e^{-\gamma\mathcal{L}}\hat{I}_m^+ + e^{\gamma\mathcal{L}}\hat{I}_m^-) \quad (7.44c)$$

$$= \hat{V}_{FT}(\mathcal{L}) + \hat{Z}\hat{T}\hat{\gamma}^{-1}(e^{-\gamma\mathcal{L}}\hat{I}_m^+ + e^{\gamma\mathcal{L}}\hat{I}_m^-)$$

The terminal constraints for the generalized Norton equivalent representation:

$$\hat{I}(0) = \hat{I}_S - \hat{\mathbf{Y}}_S \hat{V}(0) \quad (7.45a)$$

$$\hat{I}(\mathcal{L}) = -\hat{I}_L + \hat{\mathbf{Y}}_L \hat{V}(\mathcal{L}) \quad (7.45b)$$

become, substituting (7.37),

$$\hat{I}(0) = \hat{I}_S - \hat{\mathbf{Y}}_S \hat{V}(0) \quad (7.46a)$$

$$\hat{I}'(\mathcal{L}) = [-\hat{I}_L - \hat{I}_{FT}(\mathcal{L}) + \hat{\mathbf{Y}}_L \hat{V}_{FT}(\mathcal{L})] + \hat{\mathbf{Y}}_L \hat{V}'(\mathcal{L}) \quad (7.46b)$$

This shows that we can modify the equations developed for the generalized Norton equivalent in (4.95) by replacing the source  $\hat{I}_L$  with  $\hat{I}_L + \hat{I}_{FT}(\mathcal{L}) - \hat{\mathbf{Y}}_L \hat{V}_{FT}(\mathcal{L})$  and  $\hat{V}(\mathcal{L})$  with  $\hat{V}(\mathcal{L}) - \hat{V}_{FT}(\mathcal{L})$ :

$$[\hat{\Phi}_{22} \hat{\mathbf{Y}}_S + \hat{\mathbf{Y}}_L \hat{\Phi}_{11} - \hat{\Phi}_{21} - \hat{\mathbf{Y}}_L \hat{\Phi}_{12} \hat{\mathbf{Y}}_S] \hat{V}(0) \quad (7.47a)$$

$$= \underbrace{[\hat{\Phi}_{22} - \hat{\mathbf{Y}}_L \hat{\Phi}_{12}] \hat{I}_S + \hat{I}_L}_{\text{due to lumped sources}} + \underbrace{[\hat{I}_{FT}(\mathcal{L}) - \hat{\mathbf{Y}}_L \hat{V}_{FT}(\mathcal{L})]}_{\text{due to incident field}}$$

$$\hat{V}(\mathcal{L}) = \hat{V}_{FT}(\mathcal{L}) + \hat{\Phi}_{12} \hat{I}_S + (\hat{\Phi}_{11} - \hat{\Phi}_{12} \hat{\mathbf{Y}}_S) \hat{V}(0) \quad (7.47b)$$

Similarly, the alternative result given in (4.94) becomes

$$\begin{bmatrix} (\hat{Y}_s \hat{Z}_c + 1_n) \hat{\Gamma} & (\hat{Y}_s \hat{Z}_c - 1_n) \hat{\Gamma} \\ (\hat{Y}_L \hat{Z}_c - 1_n) \hat{\Gamma} e^{-j\mathcal{L}} & (\hat{Y}_L \hat{Z}_c + 1_n) \hat{\Gamma} e^{j\mathcal{L}} \end{bmatrix} \begin{bmatrix} \hat{\mathbf{I}}_m^+ \\ \hat{\mathbf{I}}_m^- \end{bmatrix} = \begin{bmatrix} \hat{\mathbf{I}}_s \\ \hat{\mathbf{I}}_L + \hat{\mathbf{I}}_{FT}(\mathcal{L}) - \hat{Y}_L \hat{V}_{FT}(\mathcal{L}) \end{bmatrix} \quad (7.48)$$

The solutions for the terminal voltages so obtained will again be given by (7.44).

The results of the mixed termination representation given in (4.96) to (4.99) are similarly obtained as

$$\begin{bmatrix} (\hat{Z}_c + \hat{Z}_s) \hat{\Gamma} & (\hat{Z}_c - \hat{Z}_s) \hat{\Gamma} \\ (\hat{Y}_L \hat{Z}_c - 1_n) \hat{\Gamma} e^{-j\mathcal{L}} & (\hat{Y}_L \hat{Z}_c + 1_n) \hat{\Gamma} e^{j\mathcal{L}} \end{bmatrix} \begin{bmatrix} \hat{\mathbf{I}}_m^+ \\ \hat{\mathbf{I}}_m^- \end{bmatrix} = \begin{bmatrix} \hat{V}_s \\ \hat{\mathbf{I}}_L + \hat{\mathbf{I}}_{FT}(\mathcal{L}) - \hat{Y}_L \hat{V}_{FT}(\mathcal{L}) \end{bmatrix} \quad (7.49)$$

or

$$\begin{aligned} & [\hat{\Phi}_{21} \hat{Z}_s + \hat{Y}_L \hat{\Phi}_{12} - \hat{\Phi}_{22} - \hat{Y}_L \hat{\Phi}_{11} \hat{Z}_s] \hat{\mathbf{I}}(0) \\ &= \underbrace{[\hat{\Phi}_{21} - \hat{Y}_L \hat{\Phi}_{11}] \hat{V}_s + \hat{\mathbf{I}}_L}_{\text{due to lumped sources}} + \underbrace{[\hat{\mathbf{I}}_{FT}(\mathcal{L}) - \hat{Y}_L \hat{V}_{FT}(\mathcal{L})]}_{\text{due to incident field}} \end{aligned} \quad (7.50a)$$

$$\hat{V}(\mathcal{L}) = \hat{V}_{FT}(\mathcal{L}) + \hat{\Phi}_{11} \hat{V}_s + (\hat{\Phi}_{12} - \hat{\Phi}_{11} \hat{Z}_s) \hat{\mathbf{I}}(0) \quad (7.50b)$$

and

$$\begin{bmatrix} (\hat{Y}_s \hat{Z}_c + 1_n) \hat{\Gamma} & (\hat{Y}_s \hat{Z}_c - 1_n) \hat{\Gamma} \\ (\hat{Z}_c - \hat{Z}_L) \hat{\Gamma} e^{-j\mathcal{L}} & (\hat{Z}_c + \hat{Z}_L) \hat{\Gamma} e^{j\mathcal{L}} \end{bmatrix} \begin{bmatrix} \hat{\mathbf{I}}_m^+ \\ \hat{\mathbf{I}}_m^- \end{bmatrix} = \begin{bmatrix} \hat{\mathbf{I}}_s \\ \hat{V}_L - \hat{V}_{FT}(\mathcal{L}) + \hat{Z}_L \hat{\mathbf{I}}_{FT}(\mathcal{L}) \end{bmatrix} \quad (7.51)$$

or

$$\begin{aligned} & [\hat{\Phi}_{12} \hat{Y}_s + \hat{Z}_L \hat{\Phi}_{21} - \hat{\Phi}_{11} - \hat{Z}_L \hat{\Phi}_{22} \hat{Y}_s] \hat{V}(0) \\ &= \underbrace{[\hat{\Phi}_{12} - \hat{Z}_L \hat{\Phi}_{22}] \hat{\mathbf{I}}_s - \hat{V}_L}_{\text{due to lumped sources}} + \underbrace{[\hat{V}_{FT}(\mathcal{L}) - \hat{Z}_L \hat{\mathbf{I}}_{FT}(\mathcal{L})]}_{\text{due to incident field}} \end{aligned} \quad (7.52a)$$

$$\hat{\mathbf{I}}(\mathcal{L}) = \hat{\mathbf{I}}_{FT}(\mathcal{L}) + \hat{\Phi}_{22} \hat{\mathbf{I}}_s + (\hat{\Phi}_{21} - \hat{\Phi}_{22} \hat{Y}_s) \hat{V}(0) \quad (7.52b)$$

**7.2.2.1 Lossless Lines in Homogeneous Media** The above final equations for determining the terminal currents and voltages of the line are considerably simplified if we assume *lossless lines in a homogeneous medium*. For this case, the per-unit-length parameter matrices satisfy

$$\mathbf{R} = 0 \quad (7.53a)$$

$$\mathbf{G} = 0 \quad (7.53b)$$

$$\mathbf{LC} = \mathbf{CL} = \mu \epsilon \mathbf{1}_n \quad (7.53c)$$

The chain parameters were derived in Chapter 4 and simplify to

$$\hat{\Phi}_{11} = \cos(\beta \mathcal{L}) \mathbf{1}_n \quad (7.54a)$$

$$\begin{aligned} \hat{\Phi}_{12} &= -jv \sin(\beta \mathcal{L}) \mathbf{L} \\ &= -j \sin(\beta \mathcal{L}) \hat{\mathbf{Z}}_C \end{aligned} \quad (7.54b)$$

$$\begin{aligned} \hat{\Phi}_{21} &= -jv \sin(\beta \mathcal{L}) \mathbf{C} \\ &= -j \sin(\beta \mathcal{L}) \hat{\mathbf{Z}}_C^{-1} \end{aligned} \quad (7.54c)$$

$$\hat{\Phi}_{22} = \cos(\beta \mathcal{L}) \mathbf{1}_n \quad (7.54d)$$

where the characteristic impedance matrix becomes real given by

$$\hat{\mathbf{Z}}_C = v \mathbf{L} \quad (7.55a)$$

$$\hat{\mathbf{Z}}_C^{-1} = v \mathbf{C} \quad (7.55b)$$

and the phase velocity of propagation in the surrounding homogeneous medium is

$$v = \frac{1}{\sqrt{\mu \epsilon}} \quad (7.56)$$

The final equations to be solved for the terminal voltages simplify considerably for this assumption. For example, consider the generalized Thévenin equivalent characterization of the terminations given in (7.42). Substituting the simplified forms of the total forcing functions,  $\hat{\mathbf{V}}_{FT}(\mathcal{L})$  and  $\hat{\mathbf{I}}_{FT}(\mathcal{L})$ , given in (7.35) and (7.36) into (7.42) gives [H.4]:

$$\begin{aligned} & [\cos(\beta \mathcal{L})(\hat{\mathbf{Z}}_S + \hat{\mathbf{Z}}_L) + jv \sin(\beta \mathcal{L})(\mathbf{L} + \hat{\mathbf{Z}}_L \mathbf{C} \hat{\mathbf{Z}}_S)] \hat{\mathbf{I}}(0) \\ &= [\cos(\beta \mathcal{L}) \mathbf{1}_n + jv \sin(\beta \mathcal{L}) \hat{\mathbf{Z}}_L \mathbf{C}] \hat{\mathbf{V}}_S - \hat{\mathbf{V}}_L \\ &+ \int_0^{\mathcal{L}} \{ \cos(\beta(\mathcal{L} - \tau)) \mathbf{1}_n + jv \sin(\beta(\mathcal{L} - \tau)) \hat{\mathbf{Z}}_L \mathbf{C} \} \\ &\times \begin{bmatrix} \vdots \\ \hat{\mathbf{E}}_z^i(i\text{-th conductor}, \tau) - \hat{\mathbf{E}}_z^i(\text{reference conductor}, \tau) \\ \vdots \end{bmatrix} d\tau \\ &- \begin{bmatrix} \vdots \\ \int_a^{a'} \tilde{\mathbf{E}}_i^i \cdot d\mathbf{l} \\ \vdots \end{bmatrix}_{z=\mathcal{L}} + \{ \cos(\beta \mathcal{L}) \mathbf{1}_n + jv \sin(\beta \mathcal{L}) \hat{\mathbf{Z}}_L \mathbf{C} \} \begin{bmatrix} \vdots \\ \int_a^{a'} \tilde{\mathbf{E}}_i^i \cdot d\mathbf{l} \\ \vdots \end{bmatrix}_{z=0} \end{aligned} \quad (7.57a)$$

and

$$\begin{aligned}
 \hat{\mathbf{I}}(\mathcal{L}) = & -j\nu \sin(\beta\mathcal{L})\mathbf{C}\hat{\mathbf{V}}_s + [\cos(\beta\mathcal{L})\mathbf{1}_n + j\nu \sin(\beta\mathcal{L})\mathbf{C}\hat{\mathbf{Z}}_s]\hat{\mathbf{I}}(0) \quad (7.57b) \\
 & - \int_0^{\mathcal{L}} \{j\nu \sin(\beta(\mathcal{L} - \tau))\mathbf{C}\} \\
 & \times \begin{bmatrix} \vdots \\ \hat{\mathbf{E}}_z^i(i\text{-th conductor}, \tau) - \hat{\mathbf{E}}_z^i(\text{reference conductor}, \tau) \\ \vdots \end{bmatrix} d\tau \\
 & - \{j\nu \sin(\beta\mathcal{L})\mathbf{C}\} \begin{bmatrix} \vdots \\ \int_a^{a'} \vec{\mathbf{E}}_z^i \cdot d\vec{\mathbf{l}} \\ \vdots \end{bmatrix}_{z=0}
 \end{aligned}$$

The generalized Norton equivalent representation in (7.47) as well as the mixed representations in (7.50) and (7.52) simplify in a similar fashion.

### 7.2.3 Lumped-Circuit Iterative Approximate Characterizations

If the line is electrically short at the frequency of the incident field, then the usual lumped-circuit, iterative approximate circuits are adequate to characterize the line. For example, the per-unit-length equivalent circuit in Fig. 7.3 as well as the MTL equations show that the Lumped  $\gamma$ ,  $\Gamma$ ,  $\pi$ , and T circuits in Fig. 4.12 can be modified to incorporate the effects of incident fields by simply multiplying the per-unit-length phasor voltage and current sources created by the incident field by the total line length, thus inserting the phasor voltage sources,  $\hat{\mathbf{V}}_{F1}\mathcal{L}$ , in series with each line self-inductance, and inserting the phasor current sources,  $\hat{\mathbf{I}}_{F1}\mathcal{L}$ , in parallel with each line self-capacitance. Since the line must be electrically short for the lumped-circuit approximation to be valid, and the cross-sectional dimensions must be electrically small for the TEM assumption to be valid, the phasor fields do not vary significantly over the line. Thus, the *per-unit-length* phasor voltage and current sources,  $\hat{\mathbf{I}}_F(z)$  in (7.24d) and  $\hat{\mathbf{V}}_F(z)$  in (7.24e), can be approximately evaluated at any convenient location on the line, say, at the center of the line. These are then multiplied by the total line length to give the lumped sources in the model. Lumped- $\pi$  and lumped-T circuits are illustrated in Fig. 7.5.

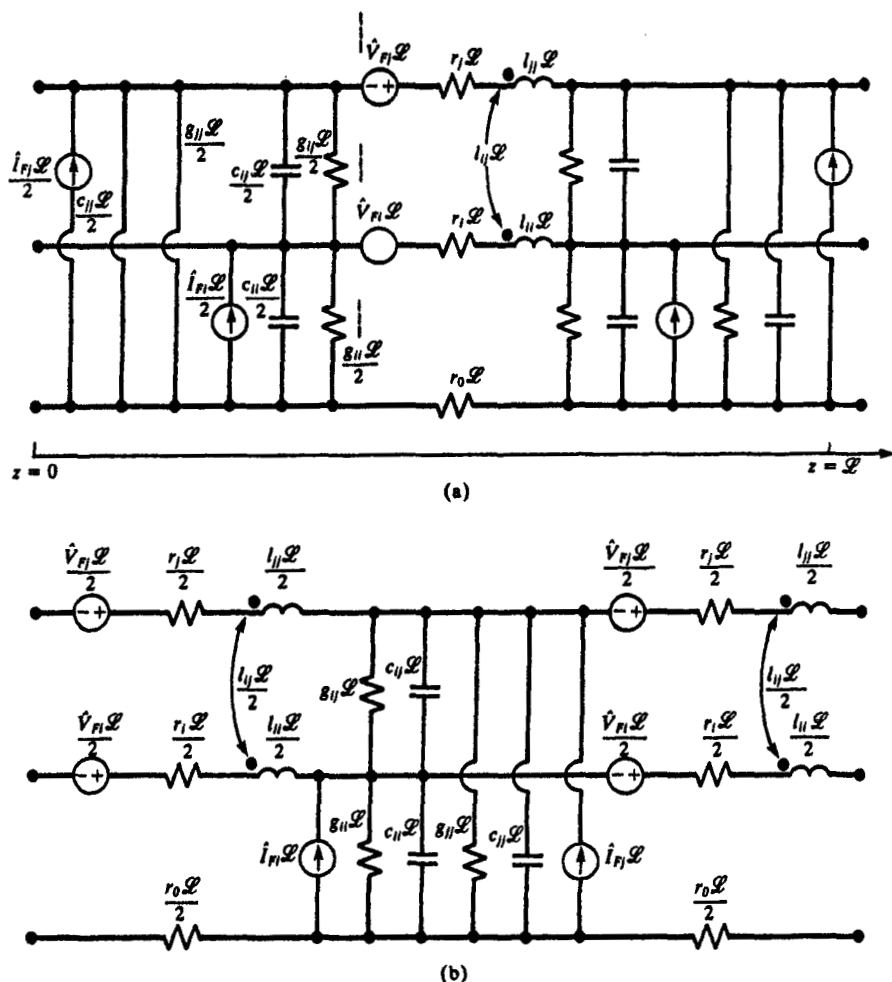


**FIGURE 7.5** Adaptation of the lumped-pi and lumped-T approximate equivalent circuits for incident-field illumination.

### 7.2.4 Uniform Plane-Wave Excitation of the Line

A significant set of problems to which these results apply is the case of illumination of the line by a *uniform plane wave* from some distant source [A.1]. The radiated fields in the far field of a radiating structure are spherical waves which locally resemble uniform plane waves. This assumption also simplifies the evaluation of the sources in the above results.

In order to characterize the frequency-domain response of the line let us describe the incident uniform plane wave angle of incidence and polarization with respect to a spherical coordinate system as illustrated in Fig. 7.6. The

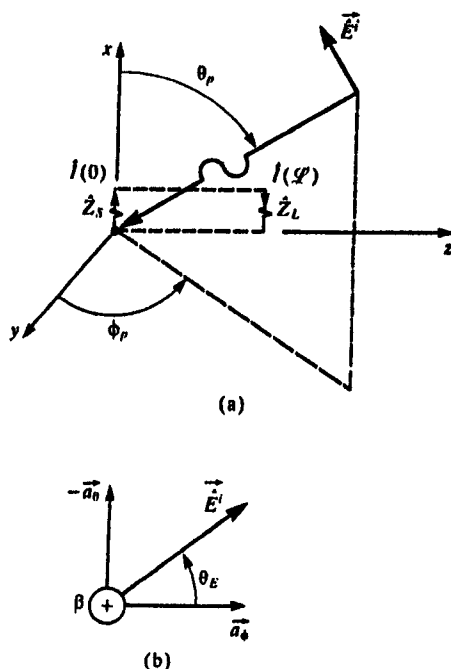


FIGURE 7.6 Definitions of the parameters characterizing the incident-field as a uniform plane wave.

propagation vector of the wave is incident on the origin of the coordinate system (the phase reference for the wave) at angles  $\theta_p$  from the  $x$  axis and  $\phi_p$  from the projection onto the  $y$ - $z$  plane from the  $y$  axis as shown in Fig. 7.6(a). The polarization of the electric field vector is described in terms of the relation to the unit vectors in the spherical coordinate system,  $\hat{a}_\theta$  and  $\hat{a}_\phi$ , as illustrated in Fig. 7.6(b). In terms of these, the general expression for the phasor electric field vector can be written as [A.1]

$$\vec{E}_i = \hat{E}_0(e_x \hat{a}_x + e_y \hat{a}_y + e_z \hat{a}_z)e^{-j\beta_x x}e^{-j\beta_y y}e^{-j\beta_z z} \quad (7.58)$$

where the components of the incident electric field vector along the  $x$ ,  $y$ , and  $z$  axes of the rectangular coordinate system describing the line are [A.1]

$$\left. \begin{aligned} e_x &= \sin \theta_E \sin \theta_p \\ e_y &= -\sin \theta_E \cos \theta_p \cos \phi_p - \cos \theta_E \sin \phi_p \\ e_z &= -\sin \theta_E \cos \theta_p \sin \phi_p + \cos \theta_E \cos \phi_p \end{aligned} \right\} \quad (7.59a)$$

and

$$e_x^2 + e_y^2 + e_z^2 = 1 \quad (7.59b)$$

The components of the phase constant along those coordinate axes are

$$\left. \begin{aligned} \beta_x &= -\beta \cos \theta_p \\ \beta_y &= -\beta \sin \theta_p \cos \phi_p \\ \beta_z &= -\beta \sin \theta_p \sin \phi_p \end{aligned} \right\} \quad (7.60)$$

The phase constant is related to the frequency and properties of the medium as

$$\begin{aligned} \beta &= \omega \sqrt{\mu \epsilon} \\ &= \frac{1}{v_o} \sqrt{\epsilon_r \mu_r} \end{aligned} \quad (7.61)$$

where  $v_o = 1/\sqrt{\mu_o \epsilon_o}$  is the phase velocity in free space and the medium is characterized by permeability,  $\mu = \mu_o \mu_r$ , and permittivity,  $\epsilon = \epsilon_o \epsilon_r$ ,  $\hat{E}_o$  is the complex amplitude of the sinusoidal wave. Although not needed, the magnetic field intensity vector of the incident wave is related to the electric field intensity vector by

$$\vec{H}^i = \frac{1}{\eta} \vec{a}_\beta \times \vec{E}^i \quad (7.62)$$

where  $\vec{a}_\beta$  is the unit vector in the direction of propagation. This gives

$$\vec{H} = \frac{1}{\eta} \hat{E}_o (h_x \vec{a}_x + h_y \vec{a}_y + h_z \vec{a}_z) e^{-j\beta_x x} e^{-j\beta_y y} e^{-j\beta_z z} \quad (7.63)$$

where the components of the incident magnetic field vector along the  $x$ ,  $y$ , and  $z$  axes of the rectangular coordinate system describing the line are [A.1]

$$\left. \begin{aligned} h_x &= -\cos \theta_E \sin \theta_p \\ h_y &= \cos \theta_E \cos \theta_p \cos \phi_p - \sin \theta_E \sin \phi_p \\ h_z &= \cos \theta_E \cos \theta_p \sin \phi_p + \sin \theta_E \cos \phi_p \end{aligned} \right\} \quad (7.64a)$$

and again

$$h_x^2 + h_y^2 + h_z^2 = 1 \quad (7.64b)$$

The intrinsic impedance of the medium is

$$\eta = \sqrt{\frac{\mu}{\epsilon}} = 120\pi \sqrt{\frac{\mu_r}{\epsilon_r}} \quad (7.65)$$

The phasor sources due to this incident plane wave,  $\hat{V}_{FT}(\mathcal{L})$  given in (7.35) and  $\hat{I}_{FT}(\mathcal{L})$  given in (7.36), can be easily evaluated in terms of the above results.



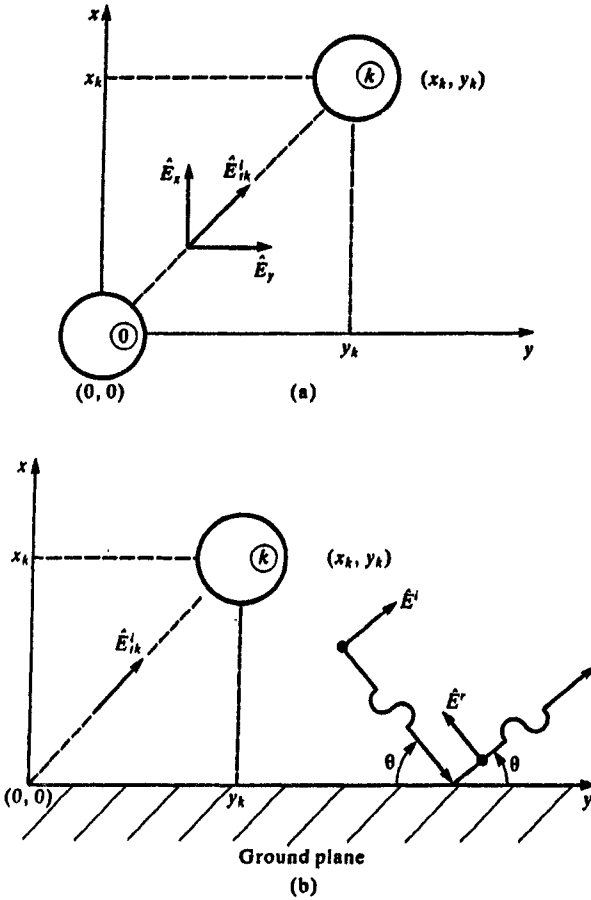


FIGURE 7.7 Derivation of the contributions to the equivalent sources due to the transverse component of the incident electric field for (a) an  $(n + 1)$ -wire line, and (b)  $n$  wires above a ground plane.

If the reference conductor is placed at the origin of the coordinate system,  $x = 0$ ,  $y = 0$ , as shown in Fig. 7.7(a), the transverse field contributions can be written in terms of the cross-sectional coordinates of the  $k$ -th conductor  $(x_k, y_k)$  using the general form of the incident field in (7.58) as

$$\hat{E}_{Tk}(\mathcal{L}) = \int_a^{a'} \tilde{\hat{E}}_{ik} \cdot d\hat{l} \quad (7.66a)$$

$$= \hat{E}_o \int_0^{d_x} \left( e_x \frac{x_k}{d_k} + e_y \frac{y_k}{d_k} \right) e^{-j\beta_z \mathcal{L}} e^{-j(\beta_x(x_k/d_k) + \beta_y(y_k/d_k))\rho} d\rho$$

$$\begin{aligned}
&= \hat{E}_o(e_x x_k + e_y y_k) e^{-j\beta_z \mathcal{L}} \frac{[e^{-j(\beta_x x_k + \beta_y y_k)} - 1]}{-j(\beta_x x_k + \beta_y y_k)} \\
&= \hat{E}_o(e_x x_k + e_y y_k) \frac{\sin(\psi_k)}{\psi_k} e^{-j\psi_k} e^{-j\beta_z \mathcal{L}}
\end{aligned}$$

where  $d_k = \sqrt{x_k^2 + y_k^2}$  is the straight-line distance between the reference conductor and the  $k$ -th conductor in the transverse plane and

$$\psi_k = \frac{(\beta_x x_k + \beta_y y_k)}{2} \quad (7.66b)$$

Similarly, the contributions due to the longitudinal field are

$$\begin{aligned}
\hat{E}_{Lk} &= \hat{E}_z^i(x_k, y_k, z) - \hat{E}_z^i(0, 0, z) \\
&= \hat{E}_o e_z e^{-j\beta_z z} [e^{-j(\beta_x x_k + \beta_y y_k)} - 1] \\
&= -j(\beta_x x_k + \beta_y y_k) \hat{E}_o e_z \frac{\sin(\psi_k)}{\psi_k} e^{-j\psi_k} e^{-j\beta_z z}
\end{aligned} \quad (7.67)$$

Substituting the expressions for the chain parameter submatrices given in (4.70):

$$\hat{\Phi}_{11}(\mathcal{L}) = \frac{1}{2} \hat{\mathbf{Y}}^{-1} \hat{\mathbf{T}} (e^{j\mathcal{L}} + e^{-j\mathcal{L}}) \hat{\mathbf{T}}^{-1} \hat{\mathbf{Y}} \quad (7.68a)$$

$$\hat{\Phi}_{21}(\mathcal{L}) = -\frac{1}{2} \hat{\mathbf{T}} \hat{\mathbf{Y}}^{-1} (e^{j\mathcal{L}} - e^{-j\mathcal{L}}) \hat{\mathbf{T}}^{-1} \hat{\mathbf{Y}} \quad (7.68b)$$

into the expressions for  $\hat{\mathbf{V}}_{FT}(\mathcal{L})$  given in (7.35) and  $\hat{\mathbf{I}}_{FT}(\mathcal{L})$  given in (7.36) yields

$$\begin{aligned}
\hat{\mathbf{V}}_{FT}(\mathcal{L}) &= \int_0^{\mathcal{L}} \frac{1}{2} \hat{\mathbf{Y}}^{-1} \hat{\mathbf{T}} (e^{j(\mathcal{L}-\tau)} + e^{-j(\mathcal{L}-\tau)}) \hat{\mathbf{T}}^{-1} \hat{\mathbf{Y}} \begin{bmatrix} \vdots \\ \hat{E}_{Lk}(\tau) \\ \vdots \end{bmatrix} d\tau \\
&\quad - \begin{bmatrix} \vdots \\ \hat{E}_{Tk}(\mathcal{L}) \\ \vdots \end{bmatrix} + \frac{1}{2} \hat{\mathbf{Y}}^{-1} \hat{\mathbf{T}} (e^{j\mathcal{L}} + e^{-j\mathcal{L}}) \hat{\mathbf{T}}^{-1} \hat{\mathbf{Y}} \begin{bmatrix} \vdots \\ \hat{E}_{Tk}(0) \\ \vdots \end{bmatrix}
\end{aligned} \quad (7.69)$$

and

$$\hat{\mathbf{I}}_{FT}(\mathcal{L}) = - \int_0^{\mathcal{L}} \frac{1}{2} \hat{\mathbf{T}} \hat{\mathbf{Y}}^{-1} (e^{j(\mathcal{L}-\tau)} - e^{-j(\mathcal{L}-\tau)}) \hat{\mathbf{T}}^{-1} \hat{\mathbf{Y}} \begin{bmatrix} \vdots \\ \hat{E}_{Lk}(\tau) \\ \vdots \end{bmatrix} d\tau \quad (7.70)$$

$$-\frac{1}{2}\hat{\mathbf{T}}\hat{\mathbf{Y}}^{-1}(\mathbf{e}^{j\mathcal{L}} - \mathbf{e}^{-j\mathcal{L}})\hat{\mathbf{T}}^{-1}\hat{\mathbf{Y}}\begin{bmatrix} \vdots \\ \hat{E}_{Tk}(0) \\ \vdots \end{bmatrix}$$

Observe that the evaluation of these forcing functions requires that we evaluate the following  $n \times 1$  vectors:

$$\hat{\mathbf{M}}^{\pm} = \int_0^{\mathcal{L}} (\mathbf{e}^{j(\mathcal{L}-\tau)} \pm \mathbf{e}^{-j(\mathcal{L}-\tau)})\hat{\mathbf{T}}^{-1}\hat{\mathbf{Y}}\begin{bmatrix} \vdots \\ \hat{E}_{Lk}(\tau) \\ \vdots \end{bmatrix} d\tau \quad (7.71)$$

and

$$\hat{\mathbf{N}}^{\pm} = (\mathbf{e}^{j\mathcal{L}} \pm \mathbf{e}^{-j\mathcal{L}})\hat{\mathbf{T}}^{-1}\hat{\mathbf{Y}}\begin{bmatrix} \vdots \\ \hat{E}_{Tk}(0) \\ \vdots \end{bmatrix} \quad (7.72)$$

The entries in these vectors become, in terms of the results in (7.66) and (7.67),

$$\begin{aligned} [\hat{\mathbf{M}}^{\pm}]_l &= \hat{E}_o e_z \left\{ e^{j_l \mathcal{L}} \frac{[1 - e^{-(j_l + j\beta_z)\mathcal{L}}]}{(j_l + j\beta_z)} \pm e^{-j_l \mathcal{L}} \frac{[e^{(j_l - j\beta_z)\mathcal{L}} - 1]}{(j_l - j\beta_z)} \right\} \\ &\times \sum_{k=1}^n \left\{ -j(\beta_x x_k + \beta_y y_k) \frac{\sin(\psi_k)}{\psi_k} e^{-j\psi_k} [\hat{\mathbf{T}}^{-1}\hat{\mathbf{Y}}]_{lk} \right\} \end{aligned} \quad (7.73)$$

where  $\psi_k$  is given by (7.66b) and

$$[\hat{\mathbf{N}}^{\pm}]_l = \hat{E}_o \{ e^{j_l \mathcal{L}} \pm e^{-j_l \mathcal{L}} \} \times \sum_{k=1}^n \left\{ (e_x x_k + e_y y_k) \frac{\sin(\psi_k)}{\psi_k} e^{-j\psi_k} [\hat{\mathbf{T}}^{-1}\hat{\mathbf{Y}}]_{lk} \right\} \quad (7.74)$$

The forcing functions in (7.69) and (7.70) become

$$\hat{\mathbf{V}}_{FT}(\mathcal{L}) = \frac{1}{2}\hat{\mathbf{Y}}^{-1}\hat{\mathbf{T}}\hat{\mathbf{M}}^{+} - \begin{bmatrix} \vdots \\ \hat{E}_{Tk}(\mathcal{L}) \\ \vdots \end{bmatrix} + \frac{1}{2}\hat{\mathbf{Y}}^{-1}\hat{\mathbf{T}}\hat{\mathbf{N}}^{+} \quad (7.75)$$

and

$$\hat{\mathbf{I}}_{FT}(\mathcal{L}) = -\frac{1}{2}\hat{\mathbf{T}}\hat{\mathbf{Y}}^{-1}\hat{\mathbf{M}}^{-} - \frac{1}{2}\hat{\mathbf{T}}\hat{\mathbf{Y}}^{-1}\hat{\mathbf{N}}^{-} \quad (7.76)$$

These results can be extended to the case where the reference conductor is an infinite, perfectly conducting ground plane illustrated in Fig. 7.7(b). The total incident field is the sum of the incident field (with the ground plane and the other conductors removed) and the reflected field. Snell's law shows that the angles of incidence and reflection are the same [A.1]. Similarly, continuity of

the tangential electric fields at the surface of the ground plane gives constraints on the  $y$  and  $z$  components of the electric field. Thus the incident and reflected (at the ground plane) fields are given by [A.1, H.1]

$$\tilde{E}^i = \hat{E}_o(e_x \hat{a}_x + e_y \hat{a}_y + e_z \hat{a}_z) e^{-j\beta_x x} e^{-j\beta_y y} e^{-j\beta_z z} \quad (7.77a)$$

$$\tilde{E}^r = \hat{E}_o(e_x \hat{a}_x - e_y \hat{a}_y - e_z \hat{a}_z) e^{j\beta_x x} e^{-j\beta_y y} e^{-j\beta_z z} \quad (7.77b)$$

Thus the total fields are

$$\hat{E}_x^{\text{total}} = \hat{E}_x^i + \hat{E}_x^r = 2\hat{E}_o e_x \cos(\beta_x x) e^{-j\beta_y y} e^{-j\beta_z z} \quad (7.78a)$$

$$\hat{E}_y^{\text{total}} = \hat{E}_y^i + \hat{E}_y^r = -2j\hat{E}_o e_y \sin(\beta_x x) e^{-j\beta_y y} e^{-j\beta_z z} \quad (7.78b)$$

$$\hat{E}_z^{\text{total}} = \hat{E}_z^i + \hat{E}_z^r = -2j\hat{E}_o e_z \sin(\beta_x x) e^{-j\beta_y y} e^{-j\beta_z z} \quad (7.78c)$$

Thus the entries in the vectors in (7.71) and (7.72) become

$$[\hat{M}^\pm]_i = -2j\hat{E}_o e_x \left\{ e^{j\gamma_i \mathcal{L}} \frac{[1 - e^{-(\gamma_i + j\beta_z)\mathcal{L}}]}{(\gamma_i + j\beta_z)} \pm e^{-j\gamma_i \mathcal{L}} \frac{[e^{(\gamma_i - j\beta_z)\mathcal{L}} - 1]}{(\gamma_i - j\beta_z)} \right\} \quad (7.79)$$

$$\times \sum_{k=1}^n \left\{ \left[ \beta_x x_k \frac{\sin(\beta_x x_k)}{\beta_x x_k} e^{-j\beta_y y_k} \right] [\hat{T}^{-1} \hat{Y}]_{ik} \right\}$$

and

$$[\hat{N}^\pm]_i = \hat{E}_o \{ e^{j\gamma_i \mathcal{L}} \pm e^{-j\gamma_i \mathcal{L}} \} \times \sum_{k=1}^n \left\{ (e_x x_k + e_y y_k) \left[ \frac{\sin(\psi_k^+)}{\psi_k^+} \right] e^{-j\psi_k \mathcal{L}} \right. \quad (7.80a)$$

$$\left. + (e_x x_k - e_y y_k) \left[ \frac{\sin(\psi_k^-)}{\psi_k^-} \right] e^{-j\psi_k \mathcal{L}} \right\} [\hat{T}^{-1} \hat{Y}]_{ik}$$

where

$$\psi_k^\pm = \beta_x x_k \pm \beta_y y_k \quad (7.80b)$$

and

$$\hat{E}_{Tk}(\mathcal{L}) = \hat{E}_o (e_x x_k + e_y y_k) \left[ \frac{\sin(\psi_k^+)}{\psi_k^+} \right] e^{-j\psi_k \mathcal{L}} e^{-j\beta_z \mathcal{L}} \quad (7.81)$$

$$+ \hat{E}_o (e_x x_k - e_y y_k) \left[ \frac{\sin(\psi_k^-)}{\psi_k^-} \right] e^{-j\psi_k \mathcal{L}} e^{-j\beta_z \mathcal{L}}$$

These results are substituted into the equations for the terminal voltages for the generalized Thévenin equivalent characterization of the terminal networks given in (7.43) and (7.44) and implemented in the FORTRAN program INCIDENT.FOR that is described in Appendix A.

### 7.2.5 Two-Conductor Lines

The previous results for a MTL are, of necessity, couched in matrix notation and are somewhat complex. In the case of a *two-conductor line* where  $n = 1$  as illustrated in Fig. 7.8, the above results simplify considerably. The chain parameter submatrices for a two-conductor line become scalars even for the most general case of a lossy line in an inhomogeneous medium, equation (4.79):

$$\hat{\phi}_{11}(\mathcal{L}) = \cosh(\hat{\gamma}\mathcal{L}) \quad (7.82a)$$

$$\hat{\phi}_{12}(\mathcal{L}) = -\sinh(\hat{\gamma}\mathcal{L})\hat{Z}_C \quad (7.82b)$$

$$\hat{\phi}_{21}(\mathcal{L}) = -\sinh(\hat{\gamma}\mathcal{L})\hat{Z}_C^{-1} \quad (7.82c)$$

$$\hat{\phi}_{22}(\mathcal{L}) = \cosh(\hat{\gamma}\mathcal{L}) \quad (7.82d)$$

where the characteristic impedance is

$$\hat{Z}_C = \sqrt{\frac{r + j\omega l}{g + j\omega c}} \quad (7.83a)$$

and the propagation constant is

$$\hat{\gamma} = \sqrt{(r + j\omega l)(g + j\omega c)} \quad (7.83b)$$

In order to simplify the notation, let us place both conductors in the  $x$ - $z$  plane parallel to the  $z$  axis as shown in Fig. 7.8. The reference conductor is placed at  $x = 0$ , and the other conductor is placed at  $x = d$ . Thus the conductors are

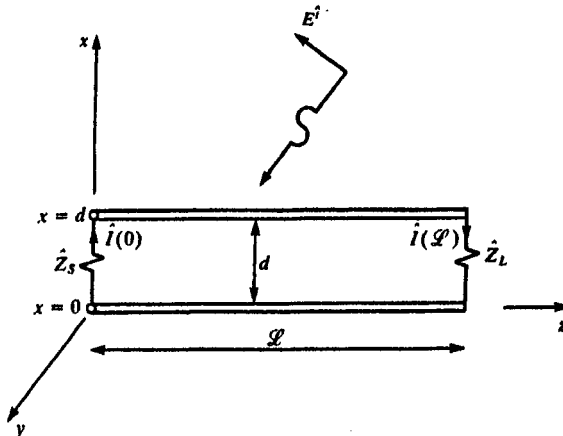


FIGURE 7.8 Definition of the line parameters for the incident-line field illumination of a two-conductor.

separated by  $d$ . Also, since the terminations are implicitly assumed to be *linear*, we will omit any lumped sources in them, i.e.,  $\hat{V}_S = \hat{V}_L = 0$ . The contributions to the terminal currents due to these lumped sources in the termination networks can be obtained with the results of Chapter 4 by superposition.

The total forcing functions due to the incident field given in (7.35) and (7.36) reduce to

$$\begin{aligned} \hat{V}_{FT}(\mathcal{L}) = & \int_0^{\mathcal{L}} \cosh(\gamma(\mathcal{L} - \tau)) [\hat{E}_z^i(d, \tau) - \hat{E}_z^i(0, \tau)] d\tau \\ & - \left[ \int_0^d \hat{E}_x^i(x, \mathcal{L}) dx \right] + \cosh(\gamma\mathcal{L}) \left[ \int_0^d \hat{E}_x^i(x, 0) dx \right] \end{aligned} \quad (7.84)$$

and

$$\begin{aligned} \hat{I}_{FT}(\mathcal{L}) = & - \int_0^{\mathcal{L}} \sinh(\gamma(\mathcal{L} - \tau)) \hat{Z}_C^{-1} [\hat{E}_z^i(d, \tau) - \hat{E}_z^i(0, \tau)] d\tau \\ & - \sinh(\gamma\mathcal{L}) \hat{Z}_C^{-1} \left[ \int_0^d \hat{E}_x^i(x, 0) dx \right] \end{aligned} \quad (7.85)$$

For  $\hat{V}_S = \hat{V}_L = 0$ , the solution for the terminal current at the source end,  $z = 0$ , for the Thévenin equivalent representation of the terminations given in (7.42a) reduces to

$$\begin{aligned} \hat{I}(0) = & \frac{\hat{V}_{FT}(\mathcal{L}) - \hat{Z}_L \hat{I}_{FT}(\mathcal{L})}{\hat{D}} \\ = & \frac{1}{\hat{D}} \int_0^{\mathcal{L}} \left[ \cosh(\gamma(\mathcal{L} - \tau)) + \sinh(\gamma(\mathcal{L} - \tau)) \frac{\hat{Z}_L}{\hat{Z}_C} \right] [\hat{E}_z^i(d, \tau) - \hat{E}_z^i(0, \tau)] d\tau \\ & - \frac{1}{\hat{D}} \left[ \int_0^d \hat{E}_x^i(x, \mathcal{L}) dx \right] \\ & + \frac{1}{\hat{D}} \left[ \cosh(\gamma\mathcal{L}) + \sinh(\gamma\mathcal{L}) \frac{\hat{Z}_L}{\hat{Z}_C} \right] \left[ \int_0^d \hat{E}_x^i(x, 0) dx \right] \end{aligned} \quad (7.86)$$

The terminal current at  $z = \mathcal{L}$  can be easily obtained from this result with the following observation. First reverse the  $z$  coordinate and add the line length,  $\mathcal{L}$ , to it, i.e., replace  $z$  with  $\mathcal{L} - z$ . This serves to reverse the roles of the terminations. Therefore, the terminal current at  $z = \mathcal{L}$  can be obtained by replacing  $z$  with  $\mathcal{L} - z$ , multiplying the equation by a minus sign (to reverse the directions of the currents), and replacing  $\hat{Z}_S$  with  $\hat{Z}_L$  and vice versa. This yields

$$\begin{aligned} \hat{f}(\mathcal{L}) = & \frac{1}{\hat{D}} \int_0^{\mathcal{L}} \left[ \cosh(\hat{\gamma}\tau) + \sinh(\hat{\gamma}\tau) \frac{\hat{Z}_s}{\hat{Z}_c} \right] [\hat{E}'_z(d, \tau) - \hat{E}'_z(0, \tau)] d\tau \quad (7.87) \\ & - \frac{1}{\hat{D}} \left[ \cosh(\hat{\gamma}\mathcal{L}) + \sinh(\hat{\gamma}\mathcal{L}) \frac{\hat{Z}_s}{\hat{Z}_c} \right] \left[ \int_0^d \hat{E}'_x(x, \mathcal{L}) dx \right] \\ & + \frac{1}{\hat{D}} \left[ \int_0^d \hat{E}'_x(x, 0) dx \right] \end{aligned}$$

The denominator in both expressions,  $\hat{D}$ , is

$$\hat{D} = \cosh(\hat{\gamma}\mathcal{L})(\hat{Z}_s + \hat{Z}_L) + \sinh(\hat{\gamma}\mathcal{L}) \left( \hat{Z}_c + \frac{\hat{Z}_s \hat{Z}_L}{\hat{Z}_c} \right) \quad (7.88)$$

These results agree with those obtained by Smith [5].

**7.2.5.1 Uniform Plane-Wave Excitation of the Line** In the case of uniform plane-wave excitation of the line with the incident electric field described by (7.58) to (7.61), the terminal current at  $z = 0$  becomes

$$\begin{aligned} \hat{f}(0) = & \frac{d\hat{E}_o}{\hat{D}} e^{-j\beta_x d/2} \left[ \frac{\sin\left(\frac{\beta_x d}{2}\right)}{\frac{\beta_x d}{2}} \right] \quad (7.89) \\ & \times \left\{ -j\beta_x e_z \int_0^{\mathcal{L}} \left[ \cosh(\hat{\gamma}(\mathcal{L} - \tau)) + \sinh(\hat{\gamma}(\mathcal{L} - \tau)) \frac{\hat{Z}_L}{\hat{Z}_c} \right] e^{-j\beta_x \tau} d\tau \right. \\ & \left. + e_x \left[ \cosh(\hat{\gamma}\mathcal{L}) + \sinh(\hat{\gamma}\mathcal{L}) \frac{\hat{Z}_L}{\hat{Z}_c} - e^{-j\beta_x \mathcal{L}} \right] \right\} \end{aligned}$$

Similarly, the terminal current at  $z = \mathcal{L}$  becomes

$$\begin{aligned} \hat{f}(\mathcal{L}) = & \frac{d\hat{E}_o}{\hat{D}} e^{-j\beta_x d/2} \left[ \frac{\sin\left(\frac{\beta_x d}{2}\right)}{\frac{\beta_x d}{2}} \right] \quad (7.90) \\ & \times \left\{ -j\beta_x e_z \int_0^{\mathcal{L}} \left[ \cosh(\hat{\gamma}\tau) + \sinh(\hat{\gamma}\tau) \frac{\hat{Z}_s}{\hat{Z}_c} \right] e^{-j\beta_x \tau} d\tau \right. \\ & \left. + e_x \left[ 1 - \left( \cosh(\hat{\gamma}\mathcal{L}) + \sinh(\hat{\gamma}\mathcal{L}) \frac{\hat{Z}_s}{\hat{Z}_c} \right) e^{-j\beta_x \mathcal{L}} \right] \right\} \end{aligned}$$

**7.2.5.2 Special Cases** The above results, although exact and general for uniform plane-wave excitation of two-conductor lines, are somewhat complicated. In this section we will specialize those results to three cases. These are illustrated in Fig. 7.9.

The first case, illustrated in Fig. 7.9(a), is referred to as *endfire* excitation and has  $\theta_p = 90^\circ$ ,  $\phi_p = -90^\circ$ , and  $\theta_E = 90^\circ$ . Thus the wave is propagating in the  $+z$  direction with the electric field polarized in the  $+x$  direction. For this incidence and polarization,

$$\left. \begin{aligned} e_x &= 1 \\ e_y &= 0 \\ e_z &= 0 \end{aligned} \right\} \quad (7.91a)$$

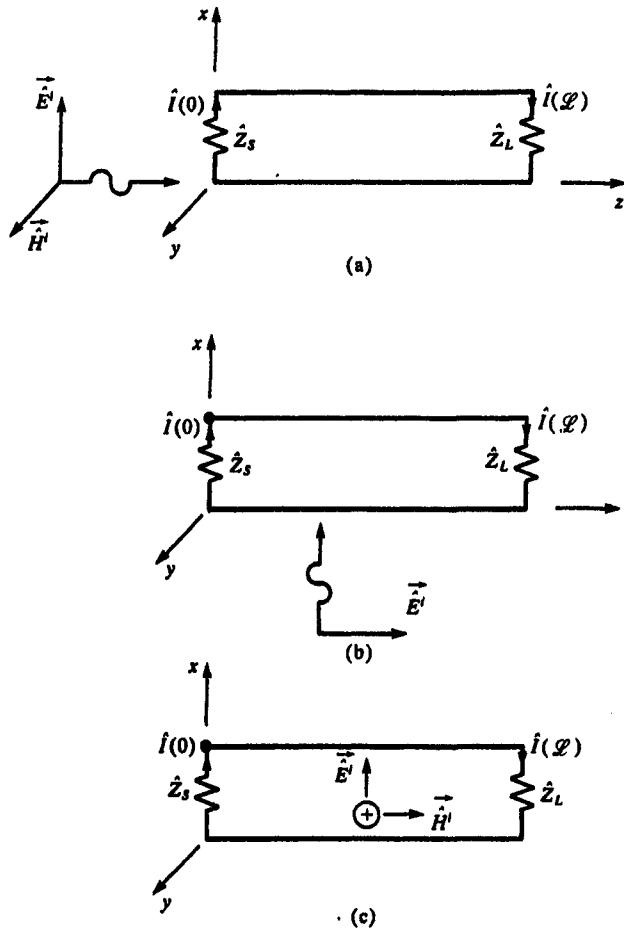


**FIGURE 7.9** Three important cases of wave incidence: (a) endfire, (b) sidefire, and (c) broadside.



and the components of the phase constant along those coordinate axes are

$$\left. \begin{aligned} \beta_x &= 0 \\ \beta_y &= 0 \\ \beta_z &= \beta \end{aligned} \right\} \quad (7.91b)$$

as expected. The complete expression for the electric field vector is, from (7.58),

$$\vec{E}^i = \hat{E}_o e^{-j\beta z} \hat{a}_x \quad (7.92)$$

Substituting these into (7.89) and (7.90) and evaluating gives

$$\hat{f}(0) = \frac{d\hat{E}_o}{\hat{D}} \left[ \cosh(\gamma \mathcal{L}) + \sinh(\gamma \mathcal{L}) \frac{\hat{Z}_L}{\hat{Z}_C} - \cos(\beta \mathcal{L}) + j \sin(\beta \mathcal{L}) \right] \quad (7.93)$$

$$\hat{f}(\mathcal{L}) = \frac{d\hat{E}_o}{\hat{D}} \left[ 1 - \left( \cosh(\gamma \mathcal{L}) + \sinh(\gamma \mathcal{L}) \frac{\hat{Z}_S}{\hat{Z}_C} \right) (\cosh(\beta \mathcal{L}) - j \sin(\beta \mathcal{L})) \right] \quad (7.94)$$

In the case of a lossless, homogeneous medium,

$$\gamma = j\beta \quad (7.95a)$$

$$\hat{Z}_C = \sqrt{\frac{l}{c}} \quad (7.95b)$$

these simplify to

$$\hat{f}(0) = j \frac{d\hat{E}_o}{\hat{D}} \sin(\beta \mathcal{L}) \left( 1 + \frac{\hat{Z}_L}{\hat{Z}_C} \right) \quad (7.96)$$

$$\hat{f}(\mathcal{L}) = \frac{d\hat{E}_o}{2\hat{D}} \left( 1 - \frac{\hat{Z}_S}{\hat{Z}_C} \right) [1 - \cos(2\beta \mathcal{L}) + j \sin(2\beta \mathcal{L})] \quad (7.97)$$

The next case, illustrated in Fig. 7.9(b), is referred to as *sidefire* excitation and has  $\theta_p = 180^\circ$ ,  $\phi_p = 0^\circ$ , and  $\theta_E = 0^\circ$ . Thus the wave is propagating in the  $+x$  direction with the electric field polarized in the  $+z$  direction. For this incidence and polarization,

$$\left. \begin{aligned} e_x &= 0 \\ e_y &= 0 \\ e_z &= 1 \end{aligned} \right\} \quad (7.98a)$$

and the components of the phase constant along those coordinate axes are

$$\left. \begin{aligned} \beta_x &= \beta \\ \beta_y &= 0 \\ \beta_z &= 0 \end{aligned} \right\} \quad (7.98b)$$

as expected. The complete expression for the electric field vector is, from (7.58),

$$\vec{E}^i = \hat{E}_o e^{-j\beta x} \hat{a}_x \quad (7.99)$$

Substituting these into (7.89) and (7.90) and evaluating gives

$$\hat{f}(0) = -j2 \frac{\hat{E}_o}{\hat{\gamma} \hat{D}} e^{-j\beta d/2} \sin\left(\frac{\beta d}{2}\right) \left[ \frac{\hat{Z}_L}{\hat{Z}_C} (\cosh(\hat{\gamma} \mathcal{L}) - 1) + \sinh(\hat{\gamma} \mathcal{L}) \right] \quad (7.100)$$

$$\hat{f}(\mathcal{L}) = -j2 \frac{\hat{E}_o}{\hat{\gamma} \hat{D}} e^{-j\beta d/2} \sin\left(\frac{\beta d}{2}\right) \left[ \sinh(\hat{\gamma} \mathcal{L}) + (\cosh(\hat{\gamma} \mathcal{L}) - 1) \frac{\hat{Z}_S}{\hat{Z}_C} \right] \quad (7.101)$$

In the case of a lossless, homogeneous medium, these simplify to

$$\hat{f}(0) = -\frac{\hat{E}_o}{\hat{D}} d e^{-j\beta d/2} \left[ \frac{\sin\left(\frac{\beta d}{2}\right)}{\frac{\beta d}{2}} \right] \left[ \frac{\hat{Z}_L}{\hat{Z}_C} (\cos(\beta \mathcal{L}) - 1) + j \sin(\beta \mathcal{L}) \right] \quad (7.102)$$

$$\hat{f}(\mathcal{L}) = -\frac{\hat{E}_o}{\hat{D}} d e^{-j\beta d/2} \left[ \frac{\sin\left(\frac{\beta d}{2}\right)}{\frac{\beta d}{2}} \right] \left[ j \sin(\beta \mathcal{L}) + (\cos(\beta \mathcal{L}) - 1) \frac{\hat{Z}_S}{\hat{Z}_C} \right] \quad (7.103)$$

The final case, illustrated in Fig. 7.9(c), is referred to as *broadside* excitation and has  $\theta_p = 90^\circ$ ,  $\phi_p = 0^\circ$ , and  $\theta_E = 90^\circ$ . Thus the wave is propagating in the  $-y$  direction with the electric field polarized in the  $+x$  direction. For this incidence and polarization,

$$\left. \begin{aligned} e_x &= 1 \\ e_y &= 0 \\ e_z &= 0 \end{aligned} \right\} \quad (7.104a)$$

and the components of the phase constant along those coordinate axes are

$$\left. \begin{aligned} \beta_x &= 0 \\ \beta_y &= -\beta \\ \beta_z &= 0 \end{aligned} \right\} \quad (7.104b)$$

as expected. The complete expression for the electric field vector is, from (7.58), ( $y = 0$ )

$$\tilde{\mathbf{E}}^i = \hat{\mathbf{E}}_o e^{j\beta y} \hat{\mathbf{a}}_x = \hat{\mathbf{E}}_o \hat{\mathbf{a}}_x \quad (7.105)$$

Substituting these into (7.89) and (7.90) along with  $y = 0$  and evaluating gives

$$\hat{f}(0) = \frac{d\hat{\mathbf{E}}_o}{\hat{D}} \left[ \cosh(j\beta \mathcal{L}) - 1 + \sinh(j\beta \mathcal{L}) \frac{\hat{\mathbf{Z}}_L}{\hat{\mathbf{Z}}_C} \right] \quad (7.106)$$

$$\hat{f}(\mathcal{L}) = \frac{d\hat{\mathbf{E}}_o}{\hat{D}} \left[ 1 - \cosh(j\beta \mathcal{L}) - \sinh(j\beta \mathcal{L}) \frac{\hat{\mathbf{Z}}_S}{\hat{\mathbf{Z}}_C} \right] \quad (7.107)$$

In the case of a lossless, homogeneous medium, these simplify to

$$\hat{f}(0) = \frac{d\hat{\mathbf{E}}_o}{\hat{D}} \left[ \cos(\beta \mathcal{L}) - 1 + j \sin(\beta \mathcal{L}) \frac{\hat{\mathbf{Z}}_L}{\hat{\mathbf{Z}}_C} \right] \quad (7.108)$$

$$\hat{f}(\mathcal{L}) = \frac{d\hat{\mathbf{E}}_o}{\hat{D}} \left[ 1 - \cos(\beta \mathcal{L}) - j \sin(\beta \mathcal{L}) \frac{\hat{\mathbf{Z}}_S}{\hat{\mathbf{Z}}_C} \right] \quad (7.109)$$

**7.2.5.3 One Conductor Above a Ground Plane** As a final application of the results for uniform plane-wave illumination of a two-conductor line we consider the case of one conductor at a height  $h$  above an infinite, perfectly conducting ground plane as illustrated in Fig. 7.10(a). In a fashion similar to the multiconductor case considered previously, this problem can be replaced with an equivalent problem by replacing the ground plane with images as illustrated in Fig. 7.10(b). The image field can be viewed as the wave reflected by the ground plane, and the total incident field is the sum of the original field and the image or reflected field. Again, Snell's law provides that the angle of incidence and the angle of reflection are equal [A.1, H.1]. Thus the fields can be written as

$$\tilde{\mathbf{E}}^i = \hat{\mathbf{E}}_o (e_x^i \hat{\mathbf{a}}_x + e_y^i \hat{\mathbf{a}}_y + e_z^i \hat{\mathbf{a}}_z) e^{-j\beta_x x} e^{-j\beta_y y} e^{-j\beta_z z} \quad (7.110a)$$

$$\tilde{\mathbf{E}}^r = \hat{\mathbf{E}}_o (e_x^r \hat{\mathbf{a}}_x + e_y^r \hat{\mathbf{a}}_y + e_z^r \hat{\mathbf{a}}_z) e^{j\beta_x x} e^{-j\beta_y y} e^{-j\beta_z z} \quad (7.110b)$$

At the position of the ground plane,  $y = 0$ , continuity of the tangential electric

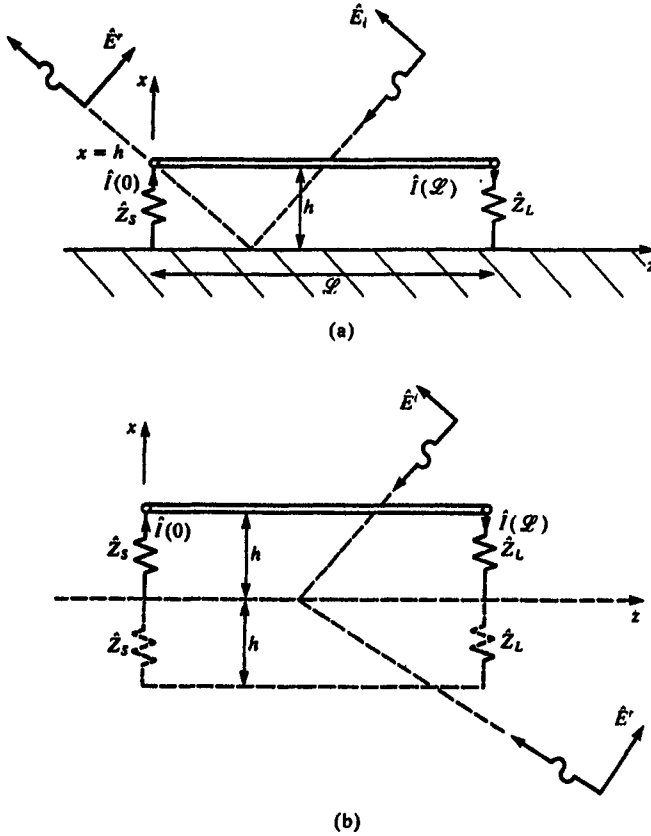


FIGURE 7.10 Replacement of the ground plane with images for incident-field illumination.

field requires that

$$e_x^r = -e_x^i \equiv -e_x \quad (7.111a)$$

$$e_y^r = -e_y^i = -e_y \quad (7.111b)$$

Thus the components of total field (incident plus reflected) can be written as (the  $y$  component is not needed)

$$\hat{E}_z^{\text{total}} = \hat{E}_z^i + \hat{E}_z^r = -j2\hat{E}_0 e_z \sin(\beta_x x) e^{-j\beta_y y} e^{-j\beta_z z} \quad (7.112a)$$

$$\hat{E}_x^{\text{total}} = \hat{E}_x^i + \hat{E}_x^r = 2\hat{E}_0 e_x \cos(\beta_x x) e^{-j\beta_y y} e^{-j\beta_z z} \quad (7.112b)$$

Equations (7.86) to (7.88) become ( $y = 0$ )

$$\hat{f}(0) = 2h \frac{\hat{E}_o}{\hat{D}} \frac{\sin(\beta_x h)}{\beta_x h} \quad (7.113)$$

$$\begin{aligned} & \times \left\{ -j\beta_x e_z \int_0^{\mathcal{L}} \left[ \cosh(\gamma(\mathcal{L} - \tau)) + \sinh(\gamma(\mathcal{L} - \tau)) \frac{\hat{Z}_L}{\hat{Z}_C} \right] e^{-j\beta_z \tau} d\tau \right. \\ & \quad \left. + e_x \left[ \cosh(\gamma\mathcal{L}) + \sinh(\gamma\mathcal{L}) \frac{\hat{Z}_L}{\hat{Z}_C} - e^{-j\beta_z \mathcal{L}} \right] \right\} \\ \hat{f}(\mathcal{L}) &= 2h \frac{\hat{E}_o}{\hat{D}} \frac{\sin(\beta_x h)}{\beta_x h} \quad (7.114) \end{aligned}$$

$$\begin{aligned} & \times \left\{ -j\beta_x e_z \int_0^{\mathcal{L}} \left[ \cosh(\gamma\tau) + \sinh(\gamma\tau) \frac{\hat{Z}_S}{\hat{Z}_C} \right] e^{-j\beta_z \tau} d\tau \right. \\ & \quad \left. + e_x \left[ 1 - \left( \cosh(\gamma\mathcal{L}) + \sinh(\gamma\mathcal{L}) \frac{\hat{Z}_S}{\hat{Z}_C} \right) e^{-j\beta_z \mathcal{L}} \right] \right\} \end{aligned}$$

Comparing (7.113) and (7.114) to (7.89) and (7.90) we see that the results for the case of a ground plane can be obtained from the case without a ground plane by removing the factor  $e^{-j\beta_x d/2}$  and replacing  $d$  with  $2h$ :  $d \Leftrightarrow 2h$ . We will find this general rule to be helpful in later results. Of course, the characteristic impedance,  $Z_C$ , in these expressions must be that of one conductor above a ground plane which is one-half the  $Z_C$  of two conductors separated by twice the height above ground (the image problem).

Again, these expressions are complicated. However, if we restrict our consideration to the special cases shown in Fig. 7.9, the results simplify. For the *endfire* excitation,  $\theta_p = 90^\circ$ ,  $\phi_p = -90^\circ$ , and  $\theta_E = 90^\circ$  we obtain  $e_x = 1$ ,  $\beta_z = \beta$ , and all others zero. The total field vector components become

$$\hat{E}_z^{\text{total}} = 0 \quad (7.115a)$$

$$\hat{E}_x^{\text{total}} = 2\hat{E}_o e^{-j\beta z} \quad (7.115b)$$

This compares to the results without the ground plane given in (7.92):

$$\hat{E}_z = 0 \quad (7.116a)$$

$$\hat{E}_x = \hat{E}_o e^{-j\beta z} \quad (7.116b)$$

Therefore we double (7.93) and (7.94) (replacing  $d = 2h$ ) which gives

$$\hat{f}(0) = \frac{2h\hat{E}_o}{\hat{D}} \left[ \cosh(\gamma\mathcal{L}) + \sinh(\gamma\mathcal{L}) \frac{\hat{Z}_L}{\hat{Z}_C} - \cos(\beta\mathcal{L}) + j \sin(\beta\mathcal{L}) \right] \quad (7.117)$$

$$\hat{f}(\mathcal{L}) = \frac{2h\hat{E}_o}{\hat{D}} \left[ 1 - \left( \cosh(\gamma\mathcal{L}) + \sinh(\gamma\mathcal{L}) \frac{\hat{Z}_S}{\hat{Z}_C} \right) (\cos(\beta\mathcal{L}) - j \sin(\beta\mathcal{L})) \right] \quad (7.118)$$

For a lossless line in a homogeneous medium, these simplify to

$$\hat{f}(0) = j \frac{2h\hat{E}_0}{\hat{D}} \sin(\beta\mathcal{L}) \left(1 + \frac{\hat{Z}_L}{\hat{Z}_C}\right) \quad (7.119)$$

$$\hat{f}(\mathcal{L}) = \frac{h\hat{E}_0}{\hat{D}} \left(1 - \frac{\hat{Z}_S}{\hat{Z}_C}\right) [1 - \cos(2\beta\mathcal{L}) + j \sin(2\beta\mathcal{L})] \quad (7.120)$$

For the *sidefire* excitation (propagating from above the ground plane in the  $-x$  direction),  $\theta_p = 0^\circ$ ,  $\phi_p = 0^\circ$ , and  $\theta_E = 0^\circ$ . For this case, we obtain  $e_x = 1$ ,  $\beta_x = -\beta$ , and all others zero. The total field vector components become

$$\hat{E}_z^{\text{total}} = j2\hat{E}_0 \sin(\beta x) \quad (7.121a)$$

$$\hat{E}_x^{\text{total}} = 0 \quad (7.121b)$$

This compares to the results without the ground plane given in (7.99):

$$\hat{E}_z = \hat{E}_0 e^{-j\beta x} \quad (7.122a)$$

$$\hat{E}_x = 0 \quad (7.122b)$$

Substituting (7.122) into (7.113) and (7.114) gives

$$\hat{f}(0) = j2h\beta \frac{\hat{E}_0}{\hat{D}} \frac{\sin(\beta h)}{\beta h} \left[ \frac{\hat{Z}_L}{\hat{Z}_C} (\cosh(j\mathcal{L}) - 1) + \sinh(j\mathcal{L}) \right] \quad (7.123)$$

$$\hat{f}(\mathcal{L}) = j2h\beta \frac{\hat{E}_0}{\hat{D}} \frac{\sin(\beta h)}{\beta h} \left[ \sinh(j\mathcal{L}) + (\cosh(j\mathcal{L}) - 1) \frac{\hat{Z}_S}{\hat{Z}_C} \right] \quad (7.124)$$

For a lossless line in a homogeneous medium, these simplify to

$$\hat{f}(0) = 2h \frac{\hat{E}_0}{\hat{D}} \frac{\sin(\beta h)}{\beta h} \left[ \frac{\hat{Z}_L}{\hat{Z}_C} (\cos(\beta\mathcal{L}) - 1) + j \sin(\beta\mathcal{L}) \right] \quad (7.125)$$

$$\hat{f}(\mathcal{L}) = 2h \frac{\hat{E}_0}{\hat{D}} \frac{\sin(\beta h)}{\beta h} \left[ j \sin(\beta\mathcal{L}) + (\cos(\beta\mathcal{L}) - 1) \frac{\hat{Z}_S}{\hat{Z}_C} \right] \quad (7.126)$$

For the *Broadside* excitation,  $\theta_p = 90^\circ$ ,  $\phi_p = 0^\circ$  and  $\theta_E = 90^\circ$ . For this case, we obtain  $e_x = 1$ ,  $\beta_x = -\beta$  and all others zero. The total field vector components become

$$\hat{E}_z^{\text{total}} = 0 \quad (7.127a)$$

$$\hat{E}_x^{\text{total}} = 2\hat{E}_0 \quad (7.127b)$$

This compares to the results without the ground plane given in (7.105):

$$\hat{E}_z = 0 \quad (7.128a)$$

$$\hat{E}_x = \hat{E}_o \quad (7.128b)$$

Therefore we simply double the results in (7.106) to (7.109) and replace  $d = 2h$  to give

$$\hat{f}(0) = \frac{2h\hat{E}_o}{\hat{D}} \left[ \cosh(\gamma\mathcal{L}) - 1 + \sinh(\gamma\mathcal{L}) \frac{\hat{Z}_L}{\hat{Z}_C} \right] \quad (7.129)$$

$$\hat{f}(\mathcal{L}) = \frac{2h\hat{E}_o}{\hat{D}} \left[ 1 - \cosh(\gamma\mathcal{L}) - \sinh(\gamma\mathcal{L}) \frac{\hat{Z}_S}{\hat{Z}_C} \right] \quad (7.130)$$

and for a lossless, homogeneous medium,

$$\hat{f}(0) = \frac{2h\hat{E}_o}{\hat{D}} \left[ \cos(\beta\mathcal{L}) - 1 + j \sin(\beta\mathcal{L}) \frac{\hat{Z}_L}{\hat{Z}_C} \right] \quad (7.131)$$

$$\hat{f}(\mathcal{L}) = \frac{2h\hat{E}_o}{\hat{D}} \left[ 1 - \cos(\beta\mathcal{L}) - j \sin(\beta\mathcal{L}) \frac{\hat{Z}_S}{\hat{Z}_C} \right] \quad (7.132)$$

**7.2.5.4 Electrically Short Lines** The previous results are exact within the TEM mode assumption. If the line length,  $\mathcal{L}$ , is substantially less than a wavelength at the frequency of interest, i.e.,  $\mathcal{L} < \lambda = v/f$ , we can approximate the line with lumped-circuit iterative structures such as the lumped- $\pi$  or lumped-T structures containing independent sources representing the effects of the incident field. Lumped-circuit codes such as SPICE can be used to solve the resulting structures.

If the line length is significantly less than a wavelength, i.e.,  $\mathcal{L} \ll \lambda = v/f$ , a very simple but approximate model can be further developed. This model is simply the lumped-circuit model wherein the line inductances and capacitances are neglected. So long as the terminal impedances,  $\hat{Z}_S$  and  $\hat{Z}_L$ , are not significantly different from the line characteristic impedance,  $\hat{Z}_C$ , this very simple model can give adequate results with a minimum of computational effort [A.3]. This model is illustrated in Fig. 7.11. It is obtained from the per-unit-length equivalent circuit in Fig. 7.3 by omitting the per-unit-length inductance,  $l$ , and per-unit-length capacitance,  $c$ , and lumping the distributed sources representing the effect of the incident field,  $\hat{V}_F(z)\Delta z \Rightarrow \hat{V}_F(\mathcal{L}/2)\mathcal{L}$  and  $\hat{I}_F(z)\Delta z \Rightarrow \hat{I}_F(\mathcal{L}/2)\mathcal{L}$ . Since the line is assumed to be very short, electrically, we can evaluate these sources at any convenient point on the line and have arbitrarily chosen to evaluate them at a midpoint of the line. Substituting the forms of these sources

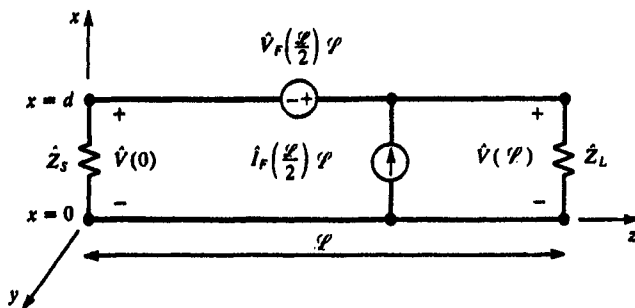


FIGURE 7.11 The low-frequency equivalent circuit for incident-field illumination.

given in (7.24) yields

$$\hat{V}_F(z)\Delta z \Rightarrow \hat{V}_F\left(\frac{\mathcal{L}}{2}\right)\mathcal{L} \quad (7.133a)$$

$$\begin{aligned} &= j\omega\mathcal{L}\left[\int_0^d \hat{B}_y(x, z) dx\right]_{z=\mathcal{L}/2} \\ &= \mathcal{L}[\hat{E}_x(d, z) - \hat{E}_x(0, z)]_{z=\mathcal{L}/2} - \mathcal{L}\frac{d}{dz}\left[\int_0^d \hat{E}_x(x, z) dx\right]_{z=\mathcal{L}/2} \end{aligned}$$

$$\hat{I}_F(z)\Delta z \Rightarrow \hat{I}_F\left(\frac{\mathcal{L}}{2}\right)\mathcal{L} \quad (7.133b)$$

$$= -j\omega c\mathcal{L}\left[\int_0^d \hat{E}_x(x, z) dx\right]_{z=\mathcal{L}/2}$$

The alternative form of (7.133a) is obtained by writing the normal magnetic field in terms of the transverse and longitudinal electric fields via (7.9) as in (7.24e). The terminal voltages can be easily obtained from the model of Fig. 7.11 using voltage division and current division as

$$\hat{V}(0) = -\frac{\hat{Z}_s}{\hat{Z}_s + \hat{Z}_L} \hat{V}_F(\mathcal{L}/2)\mathcal{L} + \frac{\hat{Z}_s\hat{Z}_L}{\hat{Z}_s + \hat{Z}_L} \hat{I}_F(\mathcal{L}/2)\mathcal{L} \quad (7.134a)$$

$$\hat{V}(\mathcal{L}) = \frac{\hat{Z}_L}{\hat{Z}_s + \hat{Z}_L} \hat{V}_F(\mathcal{L}/2)\mathcal{L} + \frac{\hat{Z}_s\hat{Z}_L}{\hat{Z}_s + \hat{Z}_L} \hat{I}_F(\mathcal{L}/2)\mathcal{L} \quad (7.134b)$$

For the case of uniform plane-wave excitation, these results can be explicitly obtained by substituting (7.58) (with  $y = 0$ ) into (7.133) to yield



$$\hat{V}_F\left(\frac{\mathcal{L}}{2}\right)\mathcal{L} = \mathcal{L}[\hat{E}_z(d, z) - \hat{E}_z(0, z)]_{z=\mathcal{L}/2} - \mathcal{L} \frac{d}{dz} \left[ \int_0^d \hat{E}_x(x, z) dx \right]_{z=\mathcal{L}/2} \quad (7.135a)$$

$$= A \hat{E}_0 \left[ \frac{\sin(\beta_x d/2)}{\beta_x d/2} \right] e^{-j\beta_x d/2} e^{-j\beta_z \mathcal{L}/2} (j\beta_z e_x - j\beta_x e_z)$$

$$\hat{I}_F\left(\frac{\mathcal{L}}{2}\right)\mathcal{L} = -j\omega c \mathcal{L} \left[ \int_0^d \hat{E}_x(x, z) dx \right]_{z=\mathcal{L}/2} \quad (7.135b)$$

$$= -j\omega c A \hat{E}_0 \left[ \frac{\sin(\beta_x d/2)}{\beta_x d/2} \right] e^{-j\beta_x d/2} e^{-j\beta_z \mathcal{L}/2} e_x$$

where the *area* of the loop formed by the conductors of the line is denoted as

$$A = d\mathcal{L} \quad (7.135c)$$

In the case of one conductor at a height  $h$  above an infinite ground plane illustrated in Fig. 7.10, using the forms of the total field given in (7.112) gives

$$\hat{V}_F\left(\frac{\mathcal{L}}{2}\right)\mathcal{L} = \mathcal{L} \left[ \hat{E}_z(h, z) - \hat{E}_z(0, z) \right]_{z=\mathcal{L}/2} - \mathcal{L} \frac{d}{dz} \left[ \int_0^h \hat{E}_x(x, z) dx \right]_{z=\mathcal{L}/2} \quad (7.136a)$$

$$= 2A \hat{E}_0 \left[ \frac{\sin(\beta_x h)}{\beta_x h} \right] e^{-j\beta_z \mathcal{L}/2} (j\beta_z e_x - j\beta_x e_z)$$

$$\hat{I}_F\left(\frac{\mathcal{L}}{2}\right)\mathcal{L} = -j\omega c \mathcal{L} \left[ \int_0^h \hat{E}_x(x, z) dx \right]_{z=\mathcal{L}/2} \quad (7.136b)$$

$$= -j\omega c 2A \hat{E}_0 \left[ \frac{\sin(\beta_x h)}{\beta_x h} \right] e^{-j\beta_z \mathcal{L}/2} e_x$$

where the loop area becomes  $A = h\mathcal{L}$ .

## 7.2.6 Computed Results

In this section we will give some computed results and compare them to results obtained by alternative methods. This will illustrate the accuracy of the formulation.

**7.2.6.1 Comparison with Predictions of the Method of Moments Codes** First we consider a lossless, two-wire transmission line with uniform plane-wave excitation [H.2]. The wires have radii of 1 mm, separations of 1 cm and total length of 1 m. The terminations at each end are identical resistors,  $\hat{Z}_S = \hat{Z}_L = R$ , with three sets of values:  $R = 552.226 \, 2 \, \Omega$  (matched loads),  $R = 50 \, \Omega$  (low-impedance

loads),  $R = 10 \text{ k}\Omega$  (high-impedance loads). Three polarizations of the incident uniform plane wave are illustrated in Fig. 7.9. The *endfire* case has the wave propagating along the line ( $z$ ) axis with the electric field vector lying in the plane of the line and polarized in the  $x$  directions:  $\tilde{E}^i = 1e^{-j\beta z}\tilde{a}_x$ . The *sidefire* case has the uniform plane wave propagating in the plane of the wires in the  $x$  direction perpendicular to them with the electric field vector polarized parallel to the wires in the  $z$  direction,  $\tilde{E}^i = 1e^{-j\beta x}\tilde{a}_z$ . The *broadside* case has the uniform plane wave propagating perpendicular to the plane of the line in the  $-y$  direction with the electric field vector polarized in the plane of the wires in the  $x$  direction,  $\tilde{E}^i = 1e^{j\beta y}\tilde{a}_x$ . Results for only certain polarizations, angles of incidence, and termination impedance values will be shown here. The reader is referred to [H.2] for more extensive numerical comparisons.

The numerical code used to give the baseline results is a method of moments (MOM) code developed at Ohio State University by J.H. Richmond [14, 15]. It will be referred to as OSMOM and uses piecewise sinusoidal expansion functions and a Galerkin technique. These features give this code exceptional accuracy. It is important to point out that the MOM method is a direct implementation of Maxwell's equations and, within numerical error, should provide "exact" solutions to compare against the predictions of the MTL model. Figure 7.12 shows the results for the endfire case and low-impedance loads ( $R = 50 \Omega$ ). Observe that the line is one wavelength long at 300 MHz so we should expect to see nulls in the frequency response at multiples of 150 MHz. Figure 7.12(a) shows the magnitude of the frequency response, whereas Fig. 7.12(b) shows the phase. Excellent correlation with the MOM results (OSMOM) are observed. The approximate, low-frequency model in (7.134) (using (7.135) with  $e_x = 1$ ,  $e_z = 0$ ,  $\beta_x = 0$ ,  $\beta_z = \beta$ ) gives a value of  $2.28 \times 10^{-5}$  at  $f = 10^7 = 10 \text{ MHz}$ . This compares with the exact value of approximately  $1.5 \times 10^{-5}$ . The error here is incurred for the following reason. Observe that the sources in (7.135) vary with frequency as  $j\omega = \omega/90^\circ$ . Therefore, the model is only valid if the magnitude of the frequency response varies linearly with frequency, 20 dB/decade, and the phase is  $\pm 90^\circ$ . This is only satisfied for frequencies below the lowest plotted frequency. Figure 7.13 shows the results for the sidefire excitation and matched loads ( $R = 552.2262 \Omega$ ), whereas Fig. 7.14 shows the results for the broadside excitation and high-impedance loads ( $R = 10 \text{ k}\Omega$ ). Excellent predictions of the MTL model are obtained for these orientations of the incident wave. The approximate low-frequency model in (7.134) (using (7.135) with  $e_x = 0$ ,  $e_z = 1$ ,  $\beta_x = \beta$ ,  $\beta_z = 0$ ) gives a value of  $1.896 \times 10^{-6}$  at  $f = 10^7 = 10 \text{ MHz}$  for the sidefire case of Fig. 7.13. This compares with the exact value of approximately  $1.9 \times 10^{-6}$ . The accuracy here is better since the frequency response clearly varies directly with frequency and the phase is  $-90^\circ$  at the lowest frequency of  $f = 10^7 = 10 \text{ MHz}$ . The approximate, low-frequency model in (7.134) (using (7.135) with  $e_x = 1$ ,  $e_z = 0$ ,  $\beta_x = \beta_z = 0$ ) gives a value of  $1.896 \times 10^{-6}$  at  $f = 10^7 = 10 \text{ MHz}$  for the broadside case of Fig. 7.14. This compares with the exact value of approximately  $9 \times 10^{-7}$ . Again, the accuracy

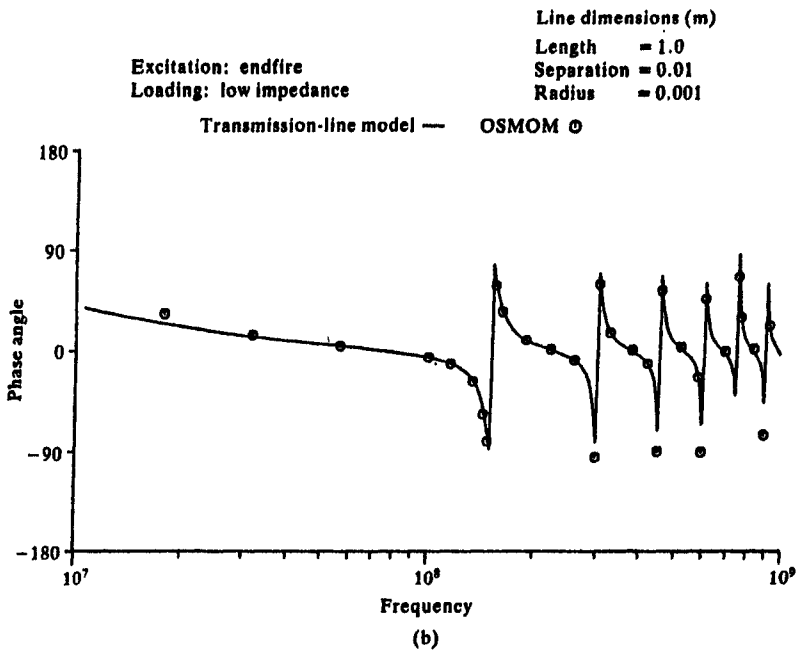
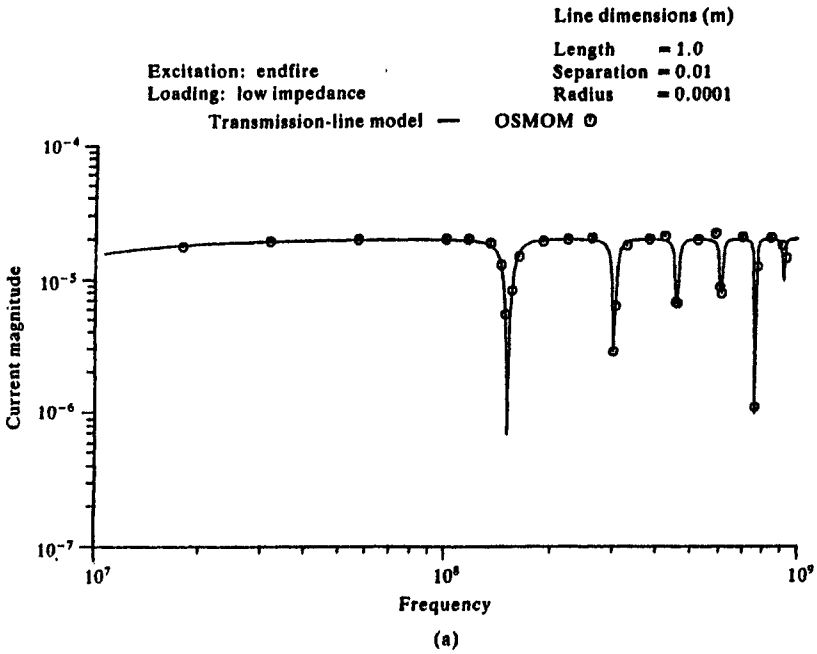


FIGURE 7.12 Comparison of the predictions of the transmission-line model and the method of moments for a two-wire line for endfire illumination: (a) magnitude, (b) phase.

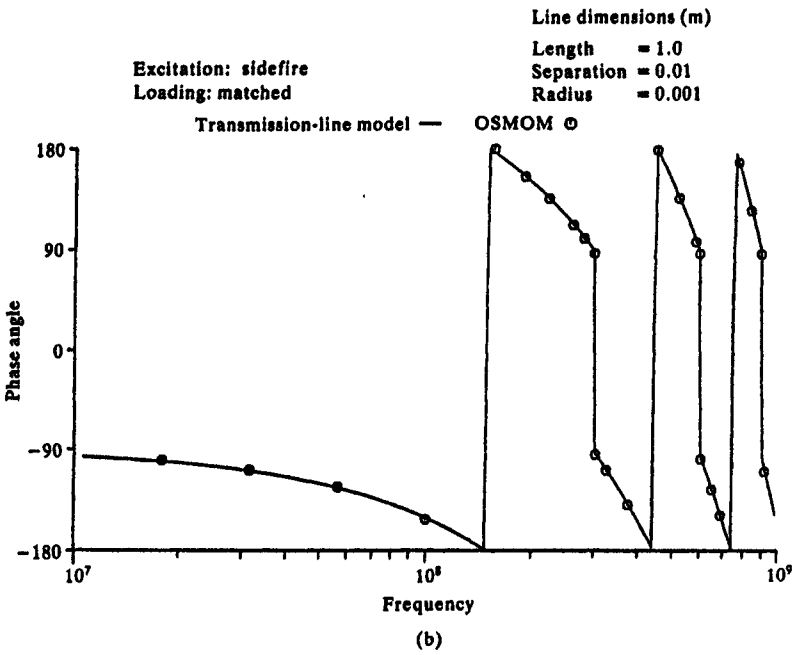
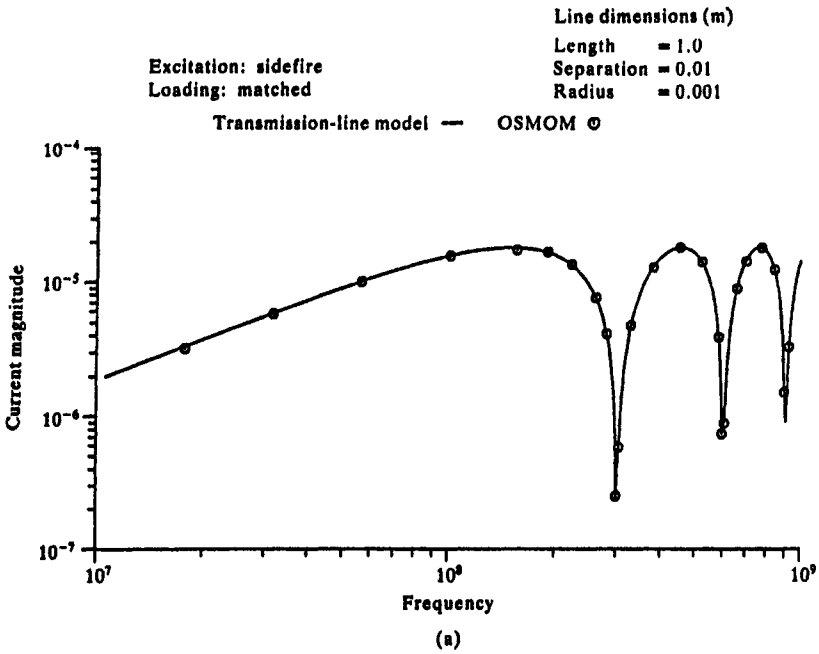
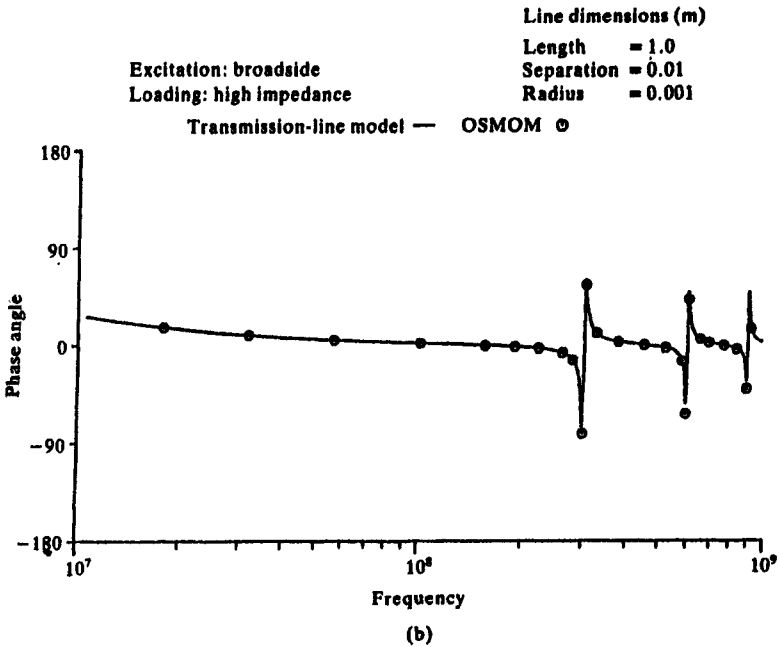
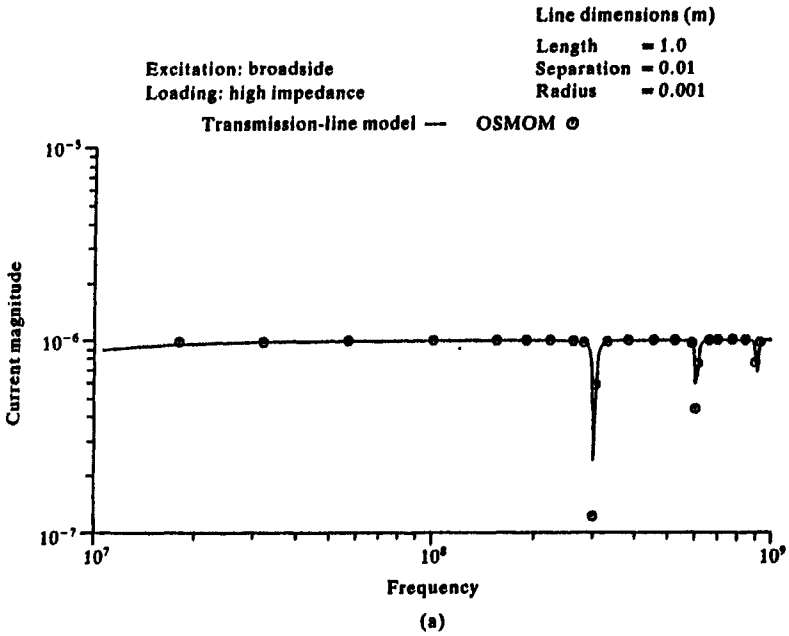


FIGURE 7.13 Comparison of the predictions of the transmission-line model and the method of moments for a two-wire line for sidefire illumination: (a) magnitude, (b) phase.



**FIGURE 7.14** Comparison of the predictions of the transmission-line model and the method of moments for a two-wire line for broadside illumination: (a) magnitude, (b) phase.

here is not as good as the sidefire case since the frequency response varies directly with frequency and the phase is  $-90^\circ$  below the lowest frequency of  $f = 10^7 = 10$  MHz. If the proper restrictions on the approximate, low-frequency model are observed, it can give reasonable estimates of the frequency response with minimal computational effort. For frequencies where the line is electrically long, we have no other recourse but to use the transmission-line model.

**7.2.6.2 A Three-Wire Line in an Incident Uniform Plane Wave** This example consists of a three-wire lossless line of length 1 m as illustrated in Fig. 7.15. The three identical wires have radii of 1 mm and lie in the  $x$ - $z$  plane. The adjacent wire separations are 1 cm, and impedances terminate each end in a star configuration. For the first case studied,  $\hat{Z}_{s0} = \hat{Z}_{s1} = \hat{Z}_{s2} = 500 \Omega$  and  $\hat{Z}_{L0} = \hat{Z}_{L1} = \hat{Z}_{L2} = 500 \Omega$ . The generalized Thévenin equivalent representation becomes

$$\hat{V}(0) = - \underbrace{\begin{bmatrix} \hat{Z}_{s1} + \hat{Z}_{s0} & \hat{Z}_{s0} \\ \hat{Z}_{s0} & \hat{Z}_{s2} + \hat{Z}_{s0} \end{bmatrix}}_{\hat{Z}_s} \hat{I}(0) = - \underbrace{\begin{bmatrix} 1000 & 500 \\ 500 & 1000 \end{bmatrix}}_{\hat{Z}_s} \hat{I}(0)$$

$$\hat{V}(\mathcal{L}) = \underbrace{\begin{bmatrix} \hat{Z}_{L1} + \hat{Z}_{L0} & \hat{Z}_{L0} \\ \hat{Z}_{L0} & \hat{Z}_{L2} + \hat{Z}_{L0} \end{bmatrix}}_{\hat{Z}_L} \hat{I}(\mathcal{L}) = - \underbrace{\begin{bmatrix} 1000 & 500 \\ 500 & 1000 \end{bmatrix}}_{\hat{Z}_L} \hat{I}(\mathcal{L})$$

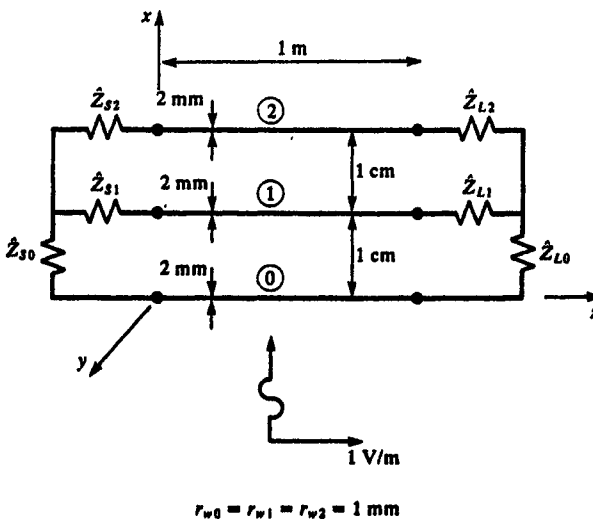


FIGURE 7.15 A three-wire line for illustration of computed results.

An incident field in the form of a uniform plane wave propagating in the  $+x$  direction with the electric field polarized in the  $+z$  direction excites the line. This problem was studied in [16], and two frequencies of the incident field were investigated:  $\beta\mathcal{L} = 1.5$  and  $\beta\mathcal{L} = 3.0$ . For the first frequency, the line is approximately  $\lambda/4$  and for the second frequency the line is approximately  $\lambda/2$ . This should provide a good test of the model since the response of MTL's tends to be the most sensitive around multiples of  $\lambda/2$ . The results computed for the line currents at  $z = 0$  by Harrison in [16] via a different technique are

$$\beta\mathcal{L} = 1.5 \begin{cases} I_0(0) = 1.766E - 5 \text{ A} \\ I_1(0) = 9.076E - 8 \text{ A} \\ I_2(0) = 1.767E - 5 \text{ A} \end{cases}$$

$$\beta\mathcal{L} = 3.0 \begin{cases} I_0(0) = 5.454E - 5 \text{ A} \\ I_1(0) = 7.736E - 7 \text{ A} \\ I_2(0) = 5.461E - 5 \text{ A} \end{cases}$$

The results computed from the distributed source MTL model described herein using the code **INCIDENT.FOR** described in Appendix A are

$$\beta\mathcal{L} = 1.5 \begin{cases} I_1(0) = 2.295\,26E - 7 / \underline{-35.636^\circ} \text{ A} \\ I_2(0) = 1.763\,62E - 5 / \underline{-109.721^\circ} \text{ A} \end{cases}$$

$$\beta\mathcal{L} = 3.0 \begin{cases} I_1(0) = 8.000E - 7 / \underline{-86.278^\circ} \text{ A} \\ I_2(0) = 5.457\,25E - 5 / \underline{-170.97^\circ} \text{ A} \end{cases}$$

which correspond well to Harrison's results.

Another result obtained by Harrison in [16] was for a 10 m line with

$$\hat{Z}_{s0} = (50 - j25) \Omega$$

$$\hat{Z}_{s1} = (100 + j100) \Omega$$

$$\hat{Z}_{s2} = (25 + j25) \Omega$$

and

$$\hat{Z}_{L0} = (50 + j25) \Omega$$

$$\hat{Z}_{L1} = (100 - j50) \Omega$$

$$\hat{Z}_{L2} = (100 - j50) \Omega$$